Lawrence Berkeley National Laboratory
Recent Work

Title

INFRARED PROPERTIES OF SOLIDS UNDER HIGH PRESSURE: CHLORINATED BENZENES AND INORGANIC CARBONATES

Permalink

https://escholarship.org/uc/item/9b26x3ps

Author

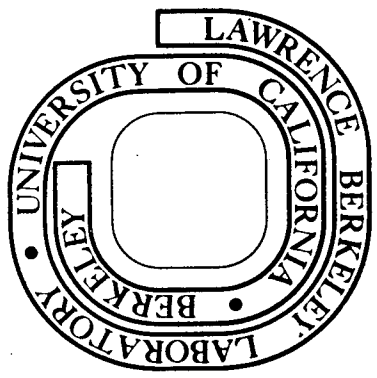Glienna, Raymond Fredric.

Publication Date

1974-09-01

INFRARED PROPERTIES OF SOLIDS UNDER HIGH PRESSURE: CHLORINATED BENZENES AND INORGANIC CARBONATES

Raymond Fredric Glienna
(Ph. D. thesis)

September, 1974

DISCLAIMER

INFRARED PROPERTIES OF SOLIDS UNDER HIGH PRESSURE;
CHLORINATED BENZENES AND INORGANIC CARBONATES

Contents

INFRARED PROPERTIES OF SOLIDS UNDER HIGH PRESSURE;
CHLORINATED BENZENES AND INORGANIC CARBONATES

Raymond Fredric Glienna

Inorganic Materials Research Division, Lawrence Berkeley Laboratory
and Department of Chemistry; University of California,
Berkeley, California

ABSTRACT

We investigate the infrared spectra of 1,2,4,5-tetrachlorobenzene, 1,4-dichlorobenzene and four naturally occurring carbonate minerals at pressures of up to 35 kilobars. Intermolecular effects manifest in the vibrational spectra are explained within the context of vibrational coupling through transition dipoles. Because of the difficulty involved in the evaluation of dipole-dipole lattice sums, we use one and two dimensional models to simulate real crystals. Results of our dipole-dipole interaction calculations are compared with the experimental data.

We also discuss the possibility of calculating bulk properties of materials through the use of their infrared spectra.

I. INTRODUCTION

The basic questions we address ourselves to in this thesis are these: first, what is the mechanism of excitonic interaction of vibrations in a molecular solid, and second, how can the interaction be described, empirically?

The infrared vibrational spectrum of a molecular solid is not much changed from that of the isolated molecules. On this basis, we can assume that the intermolecular force field in the solid provides only a small perturbation to the normal modes of vibration of the component molecules in the gas phase. A model for the intermolecular interaction as a function of molecular separation in the crystal is set up. After varying these separations (by application of high pressure), we compare experimental results with those expected from the theory.

Several workers, among them Davydov,[1] Craig and Hobbins,[2] Fox and Schnepp,[3] and Hexter,[4] have assumed that the mechanism of interaction in a molecular solid occurs primarily through a coupling of molecular transition dipoles. Agreement of experimental results with theory in this context ranges from fair to good. One of the main problems in the use of this transition dipole-transition dipole theory is the difficulty involved in calculating the interaction lattice sums in three dimensions. It has been pointed out[5,6] that such sums are only conditionally convergent in three dimensions.[*] The sums converge rapidly in one or two dimensions.

---

[*] The value of the three dimensional sums depends not only on the volume of solid considered, but also on the shape of the solid.

The task, then, is to find solids which are approximately "one or two dimensional", evaluate appropriate dipole-dipole lattice sums as functions of crystal lattice dimensions, and compare the results of these calculations with the results of high pressure-infrared optical experiments.

The solids we selected were 1,2,4,5-tetrachlorobenzene (hereafter referred to as TCB) and 1,4-dichlorobenzene (DCB). As will be explained later, TCB is considered to be a one dimensional crystal and DCB, two dimensional. We calculated dipole lattice sums for crystalline TCB and DCB and measured their infrared spectra at pressures to 35 kb.[*]

In addition, perturbations to the out-of-plane bending modes of inorganic carbonates were studied in light of a one-dimensional model by Decius.[7] We measured the bending frequencies of four naturally occurring alkaline earth carbonates to 35 kb and interpreted the results in terms of Decius' model.

For the serious reader, the following works on intermolecular interactions and on the origin and development of vibrational exciton theory are must reading; the books by Davydov[8] (translated into English by Kasha and Oppenheimer), and Craig and Walmsley,[9] and the papers by Frenkel,[10,11] Bhagavantam and Venkatarayudu,[12] Hornig,[13] Winston and Halford,[14] Craig and Hobbins,[15] and Fox and Schnepp.[16]

_____

[*]Throughout this thesis we measure pressure in kb (kilobars). One kb = 1000 bar = 987 atmospheres. Only first compression data are used.

II. THEORY

A. Effects of Molecular and Crystal Symmetry

Great simplifications to the study of molecular vibrations are (1) the assumption that purely harmonic restoring forces act upon displaced atoms and (2) the utilization of molecular symmetry properties to reduce the degree of the secular determinant to be solved. The harmonic oscillator approximation is almost universally used in normal coordinate calculations.[17] (See, however, Machida and Overend[18] and Jacobi[19,20]).

Molecular symmetry properties are very useful in conceptualizing molecular vibrations and motions and in getting a "feel" for what types of intramolecular motions will be affected by changing atomic substituents. As far as this research is concerned, symmetry properties are used to correlate motions in an isolated molecule with related motions when the molecule is condensed into the solid state.

Since this thesis does not include any actual normal coordinate calculations, we will start our discussion assuming that such normal coordinates, Q_i, can be found.[*]

Normal coordinates are defined by saying that for a molecule with N atoms

$$T = \frac{1}{2} \sum_{i=1}^{3N} (\dot{Q}_i)^2 \quad \text{and} \quad V = 2\pi^2 \sum_{i=1}^{3N} \nu_i^2 Q_i^2 \; .$$

------

[*]In fact, Scherer and Evans[21] have found sets of normal coordinates and have made an adequate assignment of the infrared and Raman spectra of TCB and DCB. The normal coordinate problem for inorganic carbonates has been solved by many workers, but see, in particular, Herzberg[22] and Donoghue, et al.[23]

That is, they are the linear combinations of 3N (mass-weighted) displacement coordinates which simultaneously reduce the molecular kinetic and potential energies to quadratic forms. ν_i is the vibrational frequency of coordinate (or mode) Q_i. These coordinates will transform according to some irreducible representation of a symmetry group which leaves the molecular energy unchanged under the various group operations.

Consider an isolated TCB or DCB molecule which belongs to the symmetry group D_{2h}. By standard group theoretical methods[24,25] we can obtain the 3N = 36 dimensional total representation of the motions of the atoms,

$$\Gamma_{total} = 6A_g + 2A_u + 2B_{1g} + 6B_{1u} + 4B_{2g} + 6B_{2u} + 6B_{3g} + 4B_{3u} \ .$$

To obtain the representation of the normal vibrations, we must subtract from Γ_{total} the motions of zero frequency, that is, the three translations and three rotations.

$$\Gamma_{vib} = \Gamma_{total} - \Gamma_{rot} - \Gamma_{trans}$$

$$\Gamma_{rot} = B_{1g} + B_{2g} + B_{3g}$$

$$\Gamma_{trans} = B_{1u} + B_{2u} + B_{3u} \ ,$$

which leaves

$$\Gamma_{vib} = 6A_g + 2A_u + B_{1g} + 5B_{1u} + 3B_{2g} + 5B_{2u} + 5B_{3g} + 3B_{3u} \ .$$

As long as we confine ourselves to electric dipole radiation, infrared transitions will be allowed to vibrational states which transform as the

irreducible representations of X, Y, or Z. The infrared fundamentals
are

$$5B_{1u} + 5B_{2u} + 3B_{3u} .$$

All are nondegenerate. The group of TCB and DCB, D_{2h}, is the direct
product of groups D_2 and i. A group character table for D_{2h} is shown
in Table I.

When TCB or DCB molecules are condensed into the solid state, they
no longer can be considered isolated. In order to characterize the
symmetry properties of the motions of a TCB or DCB molecule, we must now
examine the symmetry of the total environment around the individual
molecules.

If the crystal we are considering is finite, then it is well known[26]
that the crystal can belong to one of only 230 space groups. Here the
space group is the group of symmetry operations which carries each atom
into an identical atom and consists of point group operations, transla-
tions which generate the lattice and combinations of these operations.
Since the primitive unit cell is the smallest unit in the crystal from
which we can generate the entire crystal using only translations, we can
consider the symmetry properties of one unit cell to be characteristic
of the symmetry properties of the entire crystal. In fact, the symmetry
group of the unit cell is a factor group of the space group of the
crystal[27] with lattice translation regarded as identify. This factor
group is not generally a point group, but contains point operations,
screw axes and glide planes. Also, there are points (sites) in the
unit cell around which there is additional symmetry. The groups of

these symmetry operations (site groups) reflect the symmetry of the crystal as seen from the sites and are subgroups of the crystalline space group.*

We can give a fairly complete explanation of the modifications occurring in the vibrational spectra of a molecule or complex ion upon condensation to a solid by considering three factors. The first to be considered is the point group of the isolated molecule or ion; the second, the local or site symmetry around each molecule in the crystal; and the third, the space group of the entire crystal (or more simply, its factor group, the unit cell group).

Irreducible representations of the molecular point group are related to irreducible representations of the factor group through a "correlation diagram". Table II shows that the vibrational energy levels of TCB and DCB are split into pairs in the solid (with molecular A_u levels now allowed in infrared spectra). Also in the infrared spectra of the "aragonite-type" carbonates, the free-ion vibrational levels are split into four components (tetramolecular unit cell) with all degeneracies removed.

In order that a molecule absorb or emit electric dipole radiation in a purely vibrational transition, the integral

$$\int \psi_v \mu \psi_v' \, d\tau$$

must be nonzero. ψ_v is the ground state (totally symmetric) wave function and ψ_v' is the excited state of the vibration. μ is the

*For a complete discussion of site groups and tables showing permitted sites for most of the common space groups, see Halford.[28] However, see Couture[29] for important corrections to Halford's paper.

Table I. Group character table for symmetry group D_{2h}

	D_{2h}	E	C_{2Z}	C_{2Y}	C_{2X}	i	σ_{XY}	σ_{XZ}	σ_{YZ}
	A_g	1	1	1	1	1	1	1	1
	A_u	1	1	1	1	-1	-1	-1	-1
R_Z	B_{1g}	1	1	-1	-1	1	1	-1	-1
Z	B_{1u}	1	1	-1	-1	-1	-1	1	1
R_Y	B_{2g}	1	-1	1	-1	1	-1	1	-1
Y	B_{2u}	1	-1	1	-1	-1	1	-1	1
R_X	B_{3g}	1	-1	-1	1	1	-1	-1	1
X	B_{3u}	1	-1	-1	1	-1	1	1	-1

TCB   DCB
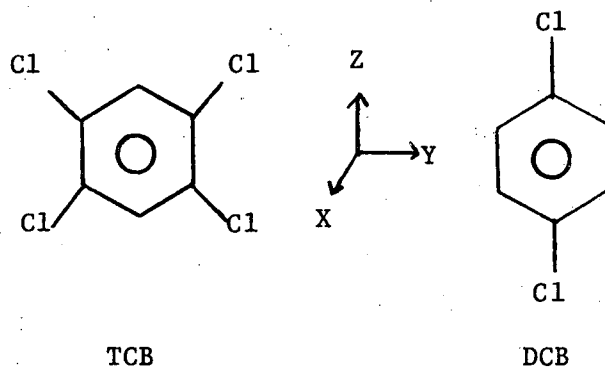
Table II. Correlation diagrams

DCB, TCB vibrations

$$\Gamma_{vib} = 6A_g + 2A_u + 5B_{1g} + 3B_{1u} + 3B_{2g} + 5B_{2u} + B_{3g} + 5B_{3u}$$

Molecular Symmetry D_{2h} Factor Group C_{2h}

	A_g	$A_g + B_g$
	A_u	$A_u + B_u$
	B_{1g}	$A_g + B_g$
(Z)	B_{1u}	$A_u + B_u$
	B_{2g}	$A_g + B_g$
(Y)	B_2u	$A_u + B_u$
	B_{3g}	$A_g + B_g$
(X)	B_{3u}	$A_u + B_u$

(a:A_u and b,c:B_u under C_{2h})

Carbonate vibrations (Aragonite-type lattice)

$$\Gamma_{vib} = A_1' + A_2'' + 2E'$$

$CO_3^=$ Symmetry D_{3h} Factor Group D_{2h}

	A_1'	$A_g + B_{1g} + B_{2u} + B_{3u}$
(Z)	A_2''	$A_u + B_{1u} + B_{2g} + B_{3g}$
(X,Y)	E'	$2(A_g + B_{1g}) + 2(B_{2u} + B_{3u})$

(a:B_{3u}, b:B_{2u} and c:B_{1u} under D_{2h})

dipole moment of the molecule. For small displacements of the atoms

within the molecule, we can expand the dipole moment in terms of the

vibrational coordinate, Q_i,

$$\mu = \mu_0 + (\frac{\partial \mu}{\partial Q_i}) Q_i + \cdots,$$

where μ_0 is the dipole moment of the molecule in its equilibrium posi-

tion. The dipole moment, μ, must belong to the same irreducible

representation as the wave function for the upper vibrational state

in order that the above integral be nonzero.

All molecules studied in this work have zero permanent dipole

moment. As an approximation, we take

$$\mu = \frac{\partial \mu}{\partial Q} \cdot Q$$

everywhere in this thesis.

B. Vibrational Exciton Theory

As a first approximation to the calculation of the ground and

first excited vibrational energy states of a molecular crystal, con-

sider the molecules to be simple one dimensional harmonic oscillators

whose centers of mass are fixed in the crystal. Define the crystal

vibrational ground state to be

$$\Phi_G = \xi_1 \xi_2 \xi_3 \cdots \xi_N .$$

There are N independent, identical oscillators (molecules) in the

crystal. Here

$$\xi_i = (\frac{4\pi\nu_i}{h})^{1/4} \exp(\frac{-4\pi^2\nu_i^2 Q_i^2}{2h}) ,$$

where Q_i is the vibrational coordinate and ν_i is the natural frequency of oscillator i. If we then assume that the oscillators can only interact pairwise with each other, the solution of the Schroedinger equation

$$\left(\sum_k H_k + \sum_{\ell>k} \sum_k V_{\ell k} \right) \Phi = E\Phi$$

gives the vibrational energy levels of the crystal. Here H_k is the Hamiltonian for an isolated harmonic oscillator k.

To the first order of perturbation theory

$$E_G = \sum_k \frac{h\nu_k}{2} + \sum_{\ell>k} \sum_k \int \xi_\ell \xi_k \, V_{\ell k} \xi_\ell \xi_k \, dQ_\ell \, dQ_k \, .$$

Upon substitution of an appropriate interaction term $V_{\ell k}$, the ground state energy can be found.

The first excited vibrational state is slightly more difficult to formulate. First define

$$\phi_p = \xi_1 \xi_2 \xi_3 \cdots \xi_p' \cdots \xi_N \, .$$

Here $\xi_1 \cdots \xi_N$ are the ground state vibrational wave functions as before, and ξ_p' is the wave function of the first excited harmonic oscillator state. Explicitly,

$$\xi_p' = \left(\frac{4\pi\nu_p^2}{\sqrt{2}\, h} \right)^{1/4} \exp\left(\frac{-4\pi^2\nu_p^2 Q_p}{2\, h} \right) H_1\left(\frac{4\pi^2\nu_p^2 Q_p}{h} \right)^{1/2} \, .$$

H_1 is the Hermite polynomial of order one. $H_1(x) = 2x$.

ϕ_p corresponds to a situation where the quantum of excitation energy is localized on oscillator p. Of course, in our approximation,

any of the N oscillators can be the one excited and we must form the following stationary states for the system

$$\Phi_r = \sum_{\ell=1}^{N} a_{r\ell} \, \phi_\ell \;.$$

Φ_r is called an exciton wave function.[30,31]

As a simple but useful example, consider the situation of N=2. Then

$$(H_1 + H_2 + V_{21}) \; \Phi = E\Phi$$

$$\Phi_G = \xi_1 \cdot \xi_2$$

$$\phi_1 = \xi_1' \cdot \xi_2$$

$$\phi_2 = \xi_1 \cdot \xi_2'$$

and

$$\Phi_1 = a_{11}\xi_1'\xi_2 + a_{12}\xi_1\xi_2'$$

$$\Phi_2 = a_{21}\xi_1'\xi_2 - a_{22}\xi_1\xi_2' \quad .$$

Remembering that $\int \xi_i \xi_j \, dQ_i \, dQ_j = \delta_{ij}$, and that different states of the same harmonic oscillator are orthogonal, we can solve for the coefficients in the Φ_r and normalize. By inspection

$$\Phi_1 = \frac{1}{\sqrt{2}} \; (\xi_1'\xi_2 + \xi_1\xi_2')$$

$$\Phi_2 = \frac{1}{\sqrt{2}} \; (\xi_1'\xi_2 - \xi_1\xi_2')$$

Then to the first order of perturbation theory (and in this case exactly)

$$E_G = \frac{h\nu_1}{2} + \frac{h\nu_2}{2} + \int \xi_1 \xi_2 V_{21} \xi_1 \xi_2 \ dQ_1 dQ_2$$

$$E_1 = \frac{3h\nu_1}{2} + \frac{h\nu_2}{2} + \frac{1}{2} \int (\xi_1' \xi_2 + \xi_1 \xi_2') V_{21} (\xi_1' \xi_2 + \xi_1 \xi_2') dQ_1 dQ_2$$

$$E_2 = \frac{h\nu_1}{2} + \frac{3h\nu_2}{2} + \frac{1}{2} \int (\xi_1' \xi_2 - \xi_1 \xi_2') V_{21} (\xi_1' \xi_2 - \xi_1 \xi_2') dQ_1 dQ_2$$

Thus, the energy levels all shift when the interaction V_{21} is "turned-on" and

$$E_2 - E_1 = 2 \int \xi_1' \xi_2 V_{21} \xi_1 \xi_2' \ .$$

The energy level separation $E_2 - E_1$ is generally termed "Davydov splitting."

Actually, the two oscillator system just described has some practical value if we consider that the two oscillators are both present in a primitive bimolecular unit cell of a crystal which is composed of a very large number of these unit cells. Then, by the Bloch theorem[32] we can construct wave functions for the whole crystal.

$$\phi^{\alpha,\beta}(k_a, k_b, k_c) = \sqrt{\frac{2}{N}} \sum_{\mu, \nu, \omega} \exp \left[i(k_a \cdot a\mu + k_b \cdot b\nu + k_c \cdot c\omega) \right]$$

$$\times \frac{1}{\sqrt{2}} (\xi_p' \xi_{p+1} \pm \xi_p \xi_{p+1}')$$

Where ϕ^{α} and ϕ^{β} are the states of even and odd symmetry, respectively.

$$0 \leqslant \mu \leqslant M_a$$

$$0 \leqslant \nu \leqslant M_b$$

$$M_a M_b M_c = \frac{N}{2} \text{ unit cells}$$

$$0 \leqslant \omega \leqslant M_c$$

$$k_a = \frac{2\pi\sigma}{M_a \cdot a} \text{ , etc.}$$

$$\sigma = 0, \pm 1, \pm 2, \ldots, \frac{M_a}{2}$$

$$\xi = \xi(\mu,\nu,\omega) \text{ and } k_a, k_b, k_c$$

are the components of the crystal wavevector $\underline{k}$. This development of

the theory can be immdeiately applied to the vast number of molecular

solids having bimolecular unit cells.

Consider the interaction of infrared radiation of frequency about

1000 cm^{-1} with a crystal having unit cell dimensions of about 5 A.

A typical Brillouin zone length is about 10^8 cm^{-1} and the wavevector

of the radiation $\underline{K}$ is, at most, about 10^4 cm^{-1}. If the absorption of

a single infrared photon by the solid creates a single phonon, then

by conservation of wavevector[33] $\underline{K}_{photon} = \underline{k}_{phonon}$, and $\underline{k}_{phonon}$ is about

10^4 cm^{-1}. This is clearly only about 1/10000 of the distance from

the zone center to a boundary in reciprocal space. For practical pur-

poses and for ease of manipulation, we can consider that the interaction

occurs at the zone center, $\underline{k}=0$.

For insight into what happens elsewhere in the Brillouin zone of

the solid chlorobenzenes, for example, see the papers by Reynolds et al.[34]

and by Swanson and Dows.[35] For two photon absorption or in cases where

a single photon promotes the system to an overtone or combination state,

the situation is considerably more complex, and the above analysis is

no longer valid.[36,37]

Now considering to first order that the interaction between pairs of molecules in a molecular solid is primarily of a dipole-dipole character,[38] we can write

$$V_{ij} = \frac{\mu_i \mu_j}{R_{ij}^3} [\hat{e}_i \cdot \hat{e}_j - 3(\hat{e}_i \cdot \hat{r}_{ij})(\hat{e}_j \cdot \hat{r}_{ij})] \tag{1}$$

where the $\hat{e}_i$ and $\hat{e}_j$ are unit vectors in the directions of dipoles i and j and the $\hat{r}_{ij}$ are unit vectors in the direction from the center of dipole (molecule) i to the center of dipole (molecule) j. μ_i and μ_j are the permanent dipole moments of dipoles i and j, and R_{ij} is the distance from the center of dipole i to the center of dipole j. Of course, this expression for the interaction of the two dipoles simply represents the electrostatic interaction of two charge distributions separated by a large distance (intermolecular distances > intramolecular distances), neglecting terms with powers of R_{ij} more negative than -3. That is, dipole-quadrupole, quadrupole-quadrupole terms, etc., are neglected. We shall discuss the validity of this approximation as applied to our experimental solids later.

For molecules with no permanent dipole moment, the interaction will occur through transition dipole moments. In this case, the total interaction energy of $n\sigma = N$ oscillators will be

$$V = \frac{1}{2} \sum_{n\alpha,m\beta}' R_{n\alpha,m\beta}^{-3} [\bar{P}_{n\alpha} \cdot \bar{P}_{m\beta} - 3(\bar{P}_{n\alpha} \cdot \hat{r}_{n\alpha,m\beta})(\bar{P}_{m\beta} \cdot \hat{r}_{n\alpha,m\beta})] \tag{2}$$

where $\bar{P}_{n\alpha} = e\sqrt{f}\,\hat{e}_\alpha$ is the effective dipole moment of the oscillator at site α of unit cell n. e is the electronic charge and f is the oscillator strength.[39] The "primed" sum means that the value zero is assigned

to the case of an oscillator interacting with itself.

For the situation where two oscillators occupy the unit cell, Davydov[40] solves for the vibrational frequencies of a solid within the context of a dipole-dipole interaction and wavevector equal to zero.

$$\nu_1^2 = \nu_o^2 + \frac{\Gamma_{11}}{4\pi^2 c^2} + \frac{\Gamma_{12}}{4\pi^2 c^2}$$

$$\nu_2^2 = \nu_o^2 + \frac{\Gamma_{11}}{4\pi^2 c^2} - \frac{\Gamma_{12}}{4\pi^2 c^2}$$

Here ν_o is the harmonic frequency of the isolated oscillator and

$$\Gamma_{11} = \sum_m{}' \frac{fe^2}{R_{m_1,m_1}^3} [(\hat{e}_1 \cdot \hat{e}_1) - 3(\hat{e}_1 \cdot \hat{r}_{n_1,m_1})(\hat{e}_1 \cdot \hat{r}_{n_1,m_1})] \tag{3}$$

$$\Gamma_{12} = \sum_m \frac{fe^2}{R_{m_1,m_2}^3} [(\hat{e}_1 \cdot \hat{e}_2) - 3(\hat{e}_1 \cdot \hat{r}_{n_1,m_2})(\hat{e}_2 \cdot \hat{r}_{n_1,m_2})] \tag{4}$$

Therefore, where identical, independent oscillators have vibrational frequency ν_o, when a dipole-dipole interaction among the oscillators is "turned-on", two vibrational frequencies arise as a result of "double occupancy" of each unit cell. Then

$$\nu_1 \simeq \nu_S [1 + \frac{1}{8\pi^2 c^2 \nu_S^2} (\Gamma_{11} + \Gamma_{12})] \tag{5}$$

$$\nu_2 \simeq \nu_S [1 + \frac{1}{8\pi^2 c^2 \nu_S^2} (\Gamma_{11} - \Gamma_{12})] \tag{6}$$

if the interaction is only a small perturbation to the system. Clearly,
we can calculate the splittings and shifts of oscillator frequencies
that occur when isolated oscillators are condensed into a solid having
a bimolecular unit cell. Also from Davydov[40] the ratio of the intensities
of the absorption bands occurring at ν_1 and ν_2 is

$$\frac{I(\nu_1)}{I(\nu_2)} = \frac{(\hat{e}_1 + \hat{e}_2)^2}{(\hat{e}_1 - \hat{e}_2)^2} \tag{7}$$

In going from this model to a real crystalline solid, we must
assume that at each lattice site in the solid there is no longer simply
a one dimensional harmonic oscillator, but a molecule with $3n-6$ normal
modes of vibration, where n is the number of atoms in the molecule.
The theory is not effectively changed, however, because there is ample
evidence[41] that only like normal modes of different molecules interact.
But, of course, we must make each ξ_i into a product of $3n-6$ simple
harmonic oscillator wave functions.

This theory will be illustrated in detail in the calculations done
on the crystalline chlorobenzenes and on inorganic carbonates.

III. INSTRUMENTATION

A. Background

Some of the first optical experiments performed on samples subject to high pressure were done by Fishman and Drickamer[42] in 1956. They studied the optical properties of solutions at pressures to twelve kb using a sapphire cell. Their cell operated under hydrostatic conditions and was nearly ideal for studying high pressure properties of solutions over a wide spectral range. The synthetic sapphires used were essentially transparent in the frequency range 50,000 cm^{-1} to 2,000 cm^{-1}.

In experimental studies of molecular and ionic compounds, Weir, et al.[43,44] used diamond squeezers to hold solid samples at a high pressure while the spectral regions down to 700 cm^{-1} and in some cases even 285 cm^{-1} were investigated. Diamond squeezers provide a very efficient means of application of a large stress to a sample, but the stress applied is necessarily uniaxial. Large pressure gradients are generated in the samples broadening absorption lines and leaving uncertain what "pressure" the sample is actually under in the region of observation. The pressure varies from zero to four times average in the cell center.[45] An added drawback is that both type I and type II diamonds have strong spectral absorptions in the region 2,500 cm^{-1} to 1,600 cm^{-1}.

In 1960, Balchan and Drickamer[46] invented cells using NaCl as the pressure transmitting medium, pressure support material, and optical window. One of the cells was usable to nominal pressures of 50 kb and the other to about 200 kb. The original application of the cells was in the visible and ultraviolet regions of the spectrum, but extension

was made both into the infrared in absorption experiments, and great
use was made of the cells in Raman and Rayleigh scattering experiments.[47,48]
Other cells were used by Ferraro,[49,50] Gebbie et al.,[51] and Sherman.[52]

B. High Pressure Cell

We shall discuss only the first of the so-called "Drickamer" cells
because it is one of the simplest, well-suited to our optical equipment
and the cell used throughout this work. It is shown in cross-section
in Fig. 1. The cell used in this study was kindly provided by Professor
Malcolm Nicol of UCLA and is described briefly below. For details see
Nicol et al.[53]

The cell consists of an inner tool steel insert surrounded by an
outer steel jacket. The sample chamber is a hole of 0.318 cm diameter
ground into the center of the insert. The optical path through the
cell consists of a series of concentric holes drilled symmetrically into
either side. The smallest hole in the steel jacket is 0.635 cm in
diameter and 0.635 cm deep. The three sections of the optical window
in the insert are of equal length and of diameters 0.16 cm, 0.12 cm,
and 0.08 cm. The entire optical window will be filled with NaCl. The
sample chamber, thus, will be surrounded by high strength tool steel on
the entirety of its curved surface, except at the two 0.08 cm diameter
spots where support will be provided by 1.8 cm of NaCl on either side,
utilizing the principle of "massive support".[54]

The filling of the tapering optical path in the outer steel jacket
and in the tool steel insert is accomplished as follows. Single
crystals of NaCl are machined to a cylindrical shape of diameter

0.635 cm and are cut to lengths of 0.635 cm. One of these NaCl rods

is inserted into the 0.635 cm diameter hole on either side of the cell

assembly and followed by a 0.635 cm diameter steel piston. The cell

and pistons are heated to about 300°C and held at that temperature for

at least two hours. The entire assembly is removed from the oven and

a pressure of about 5-7 kb is applied to the NaCl through the pistons.

The pressure is maintained until NaCl extrudes through the holes in

the tool steel insert and into the sample chamber. When the temperature

of the cell has dropped sufficiently, the pressure is released slowly,

and the pistons are removed from the cell assembly. Any NaCl remain-

ing in the large 0.635 cm diameter holes on either side of the cell is

drilled out and the NaCl in the sample chamber is removed.

A similar NaCl rod is then inserted into either side of the cell

assembly and at ambient temperature a pressure of 5 kb is again applied

through the pistons the small diameter faces of which have been polished

to optical quality. When the pressure is released (after at least two

hours), the two sections of NaCl on either side of the assembly should

be fused together. Remove the pistons and sight along the optical path

into a lighted flashlight. If any light at all can be seen, the ap-

paratus is then ready to be used. If the light path is opaque to the

visible light, insert a machined 0.318 cm diameter NaCl cylinder into

the sample chamber and apply about 1 kb to it through tungsten carbide

pistons for an hour. Then cold press the NaCl rods in the sides of the

assembly to 5 kb for another hour. When the pressure is released and

the light path is checked for light transmission, opacity necessitates

repetition of the last two pressure applications until there is some
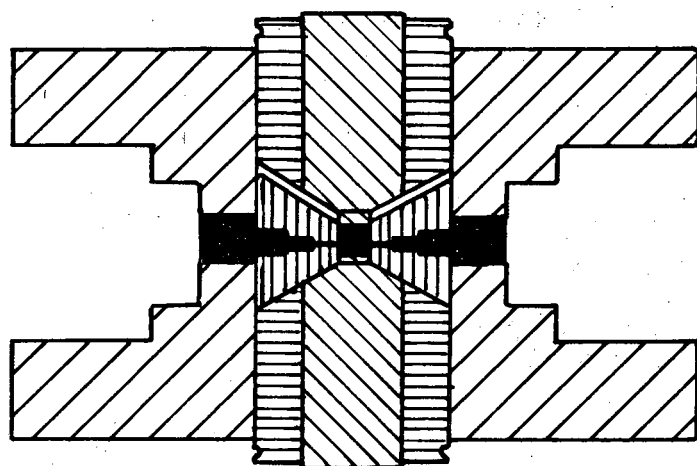
Outer steel jacket

Tool steel insert

Anvil sleeve

Tungsten carbide anvils and pistons

Na Cl

XBL 747-6831

Fig. 1. Drickamer cell.

light transmitted. If the assembly is translucent or better, it can be used almost indefinitely. The only thing that must be remembered is that a pressure of about 5 kb must be re-applied to the sides before each new sample is introduced.

When experiments are to be performed, the sample chamber is prepared in the following way. After normal cleavage planes are marked, a single NaCl crystal is machined to a diameter of 0.138 cm. It is then polished to optical quality, removed from the machining apparatus, cut to an appropriate length,* and cleaved along a normal cleavage plane containing the cylindrical axis. A single crystal, multicrystalline, or powdered sample of thickness 0.003 cm and diameter about 0.15 cm is inserted between the two cylinder halves. The rejoined NaCl cylinder is the "pressure transmitting medium". The pressure transmitting medium with sample is inserted into the sample chamber so that the light path is perpendicular to the sample. On the bottom of the pressure transmitting medium is placed a 0.076 cm thick tungsten carbide disc of diameter 0.318 cm backed up by a 0.318 cm diameter Bridgman anvil which fits the diameter and taper of the tool steel insert. The cylinder is topped by a tungsten carbide disc 0.318 cm diameter and 0.178 cm thick and another Bridgman anvil. The cell assembly is now ready to be used in a high pressure-infrared experiment.

---

*Lengths varied up to about 0.4 cm throughout this study with little effect on results as long as long as at least 0.07 cm of the top tungsten carbide piston (described above) protrudes above the tool steel insert.
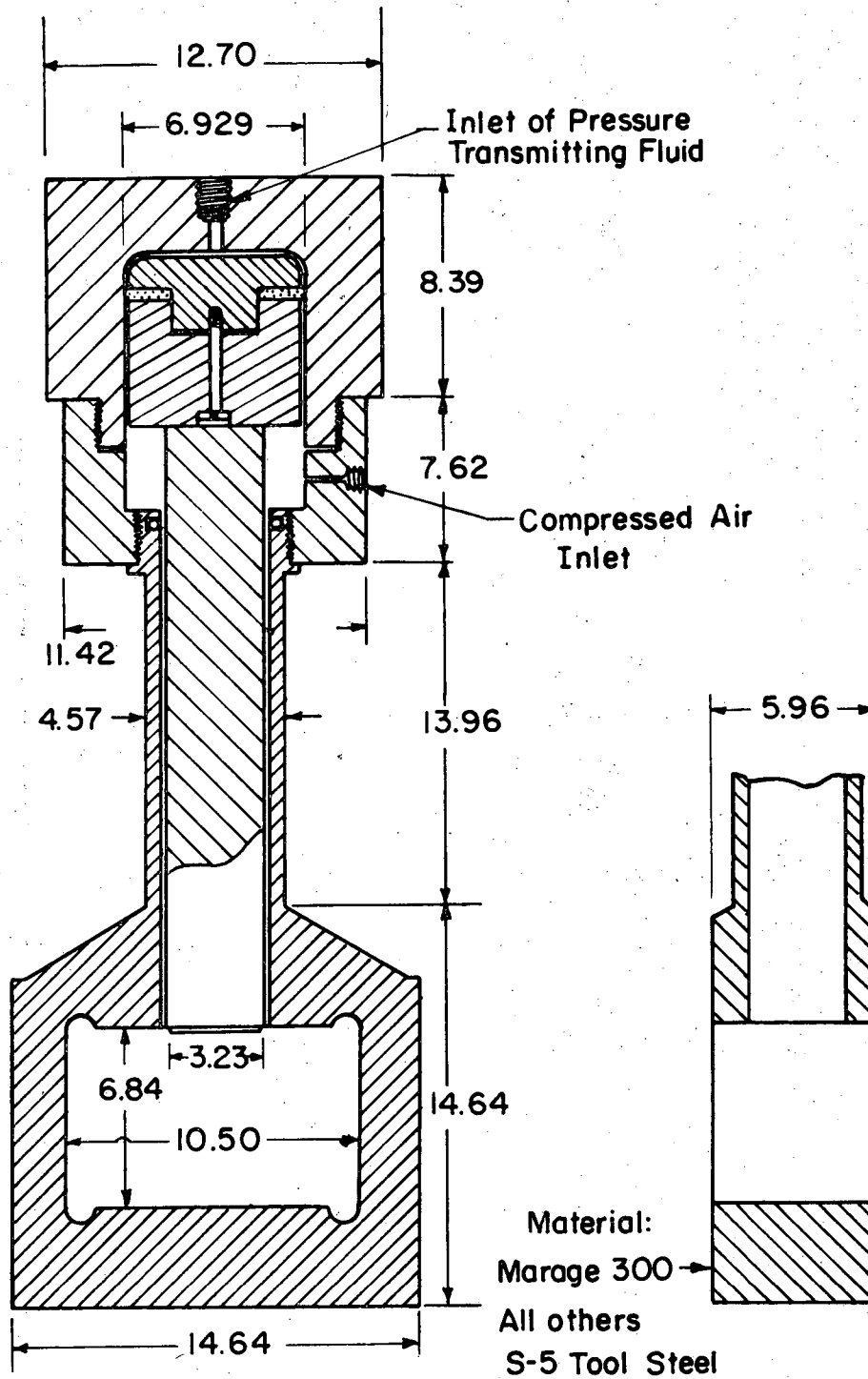
C. The Press

A small portable press was constructed by Duane Newhart in the shops of Lawrence Berkeley Laboratory and was used in this study (Fig. 2). The press is capable of applying a load of up to 3,600 kg to the 0.0792 cm^2 surface area of the sample chamber of the optical cell.

In a compression process the pressure transmitting fluid (usually #2 turbine oil) enters into the cylinder of the press above a Bridgman seal and applies a pressure to the top surface of the 6.929 cm diameter ram. The load is then transmitted to the Bridgman anvils via a 3.23 cm diameter steel bar. There is a pressure intensification on the optical cell of a factor of 476.4 over the pressure existing in the hydraulic lines. With normal use, oil pressure is constant to within 10% during the few hours required for an experimental run, but can be maintained to a few percent manually.

Final decompression to remove the optical cell is achieved by introducing compressed air into the compressed air inlet in order to raise the Bridgman seal.

D. Optics

The light source used throughout this work to provide a sample beam was a glass-jacketed, water-cooled, concentrated zirconium arc lamp (Sylvania-type 300 AC, 300 W), with a NaCl window. Such a lamp[55] is a considerably more intense source than a Globar rod,[56] but not as intense as would be expected from its higher operating temperature (Globar ~ 1175 K, Zr Arc ~ 2400 K, see Fig. 3). It is also cheap, easy to operate, and has small image size.

12.70

6.929

Inlet of Pressure
Transmitting Fluid

8.39

7.62

Compressed Air
Inlet

11.42

4.57

13.96

5.96

3.23

6.84

10.50

14.64

14.64

Material:
Marage 300
All others
S-5 Tool Steel

XBL 747-6832

Fig. 2. Hydraulic press.
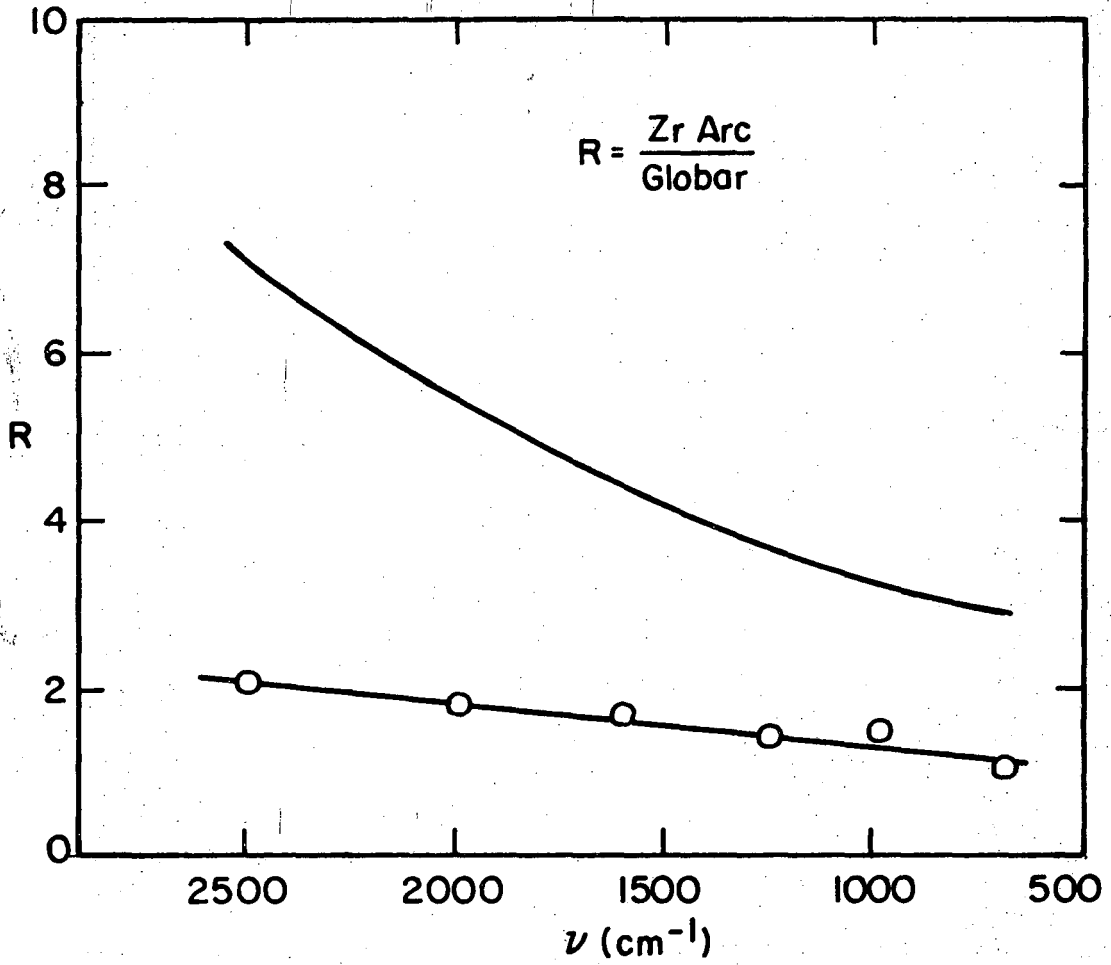
Fig. 3. Ratio of intensities of Zr arc to globar rod. Upper
curve is the ratio calculated from Black Body radiators.
Lower curve is from reference 55.

The Zr Arc is operated in the following manner. A polished NaCl window (5.5 cm diameter, 0.6 cm thick) is sealed (Blackwax) to the opening in the glass vacuum jacket around the source. The entire lamp is evacuated and flushed with a few mm Hg of argon and filled with argon to a pressure of about 200 mm Hg. The lamp is operated by commercial power supplies (at least 30 volts, 20 amperes D.C.) and is started by application of at least 2,000 volts to the cathode until ignition occurs. In ordinary operation, the lamp need not usually be refilled with argon unless difficulty is encountered in starting. If such problems arise, evacuate the lamp, refill with argon, and try for ignition again. If the lamp is still difficult to start, the cathode must be cleaned mechanically. The type 300 AC lamp has a negative volt-ampere characteristic so the circuit must be provided with suitable ballast resistance. Some typical operating conditions are

Voltage 30 volts D.C.

Current 10 amperes

Ballast 2 ohms .

Any current of less than about 15 amperes that provides satisfactory spectroscopic results is more than adequate to assure long lamp life.

The lamp is part of the external optical system shown in Fig. 4, which is similar to that used by C. K. Wu.[57] These external optics are designed for use with the optics in the monochromator compartment of a Perkin-Elmer Model 21 infrared spectrophotometer.

Diverging light from the source is collected by spherical mirror M_1 and brought to a focus at F_1. Radiation from F_1 is directed onto spherical mirror M_4 and focussed at F_2. When used properly with the
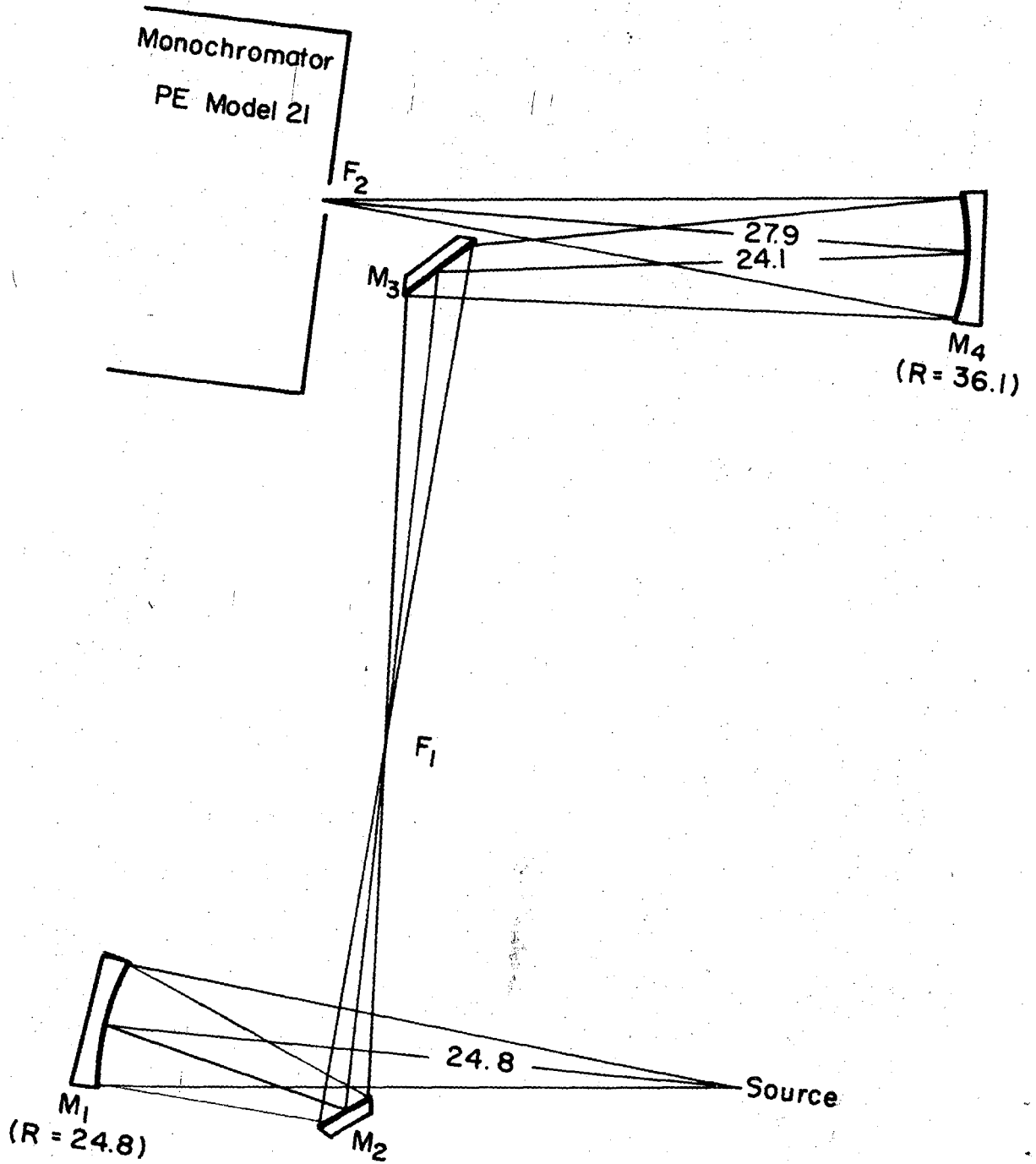
Fig. 4. External optics.

XBL 747-6830

PE 21 monochromator, these optics provide both an image of the source
at the entrance slit of the monochromator and correct aperture. Both
external and internal optics must be adjusted to keep the radiation
properly focussed and in the focal plane before each experimental run.

When experiments are performed, the high pressure optical cell
is placed such that the sample is situated at F_1. In actual practice
the distances shown in Fig. 4 must be considered approximate and ad-
justed to give maximum light transmission.   The internal system is
maintained in strict accordance with the manufacturer's instructions
and the monochromator compartment is constantly flushed with dry
nitrogen (boil-over from liquid nitrogen supply).

E. <u>Calibration of the Frequency Scale</u>

The monochromator frequency counter is calibrated using the
seventeen well-established absorption lines shown in Table III.
Figure 5 plots "error" versus frequency. The error bars are the
manufacturer's stated abscissa accuracy limits for a NaCl prism. All
frequencies are stated only to the nearest cm^{-1} because of these
accuracy limits. Correction due to the refractive index of air is
less than 1 cm^{-1} and is ignored. The frequency scale is reproducible
to at least 0.1 cm^{-1}.

Table III.   Calibration of frequency counter.

counter number (cm^{-1})	"true value" (cm^{-1})	error	
1770	1774	+4	H_2O vapor
1699	1770	+1	H_2O vapor
1638	1637	-1	H_2O vapor
1619	1618	-1	H_2O vapor
1562	1560	-2	H_2O vapor
1512	1508	-4	H_2O vapor
1493	1491	-2	H_2O vapor
1462	1459	-3	H_2O vapor
1423	1420	-3	H_2O vapor
1399	1396	-3	H_2O vapor
1341	1340	-1	H_2O vapor
1183	1181	-2	polystyrene film
1156	1154	-2	polystyrene film
1069	1069	0	polystyrene film
1028	1028	0	polystyrene film
905	907	+2	polystyrene film
730	730	0	polyethylene film
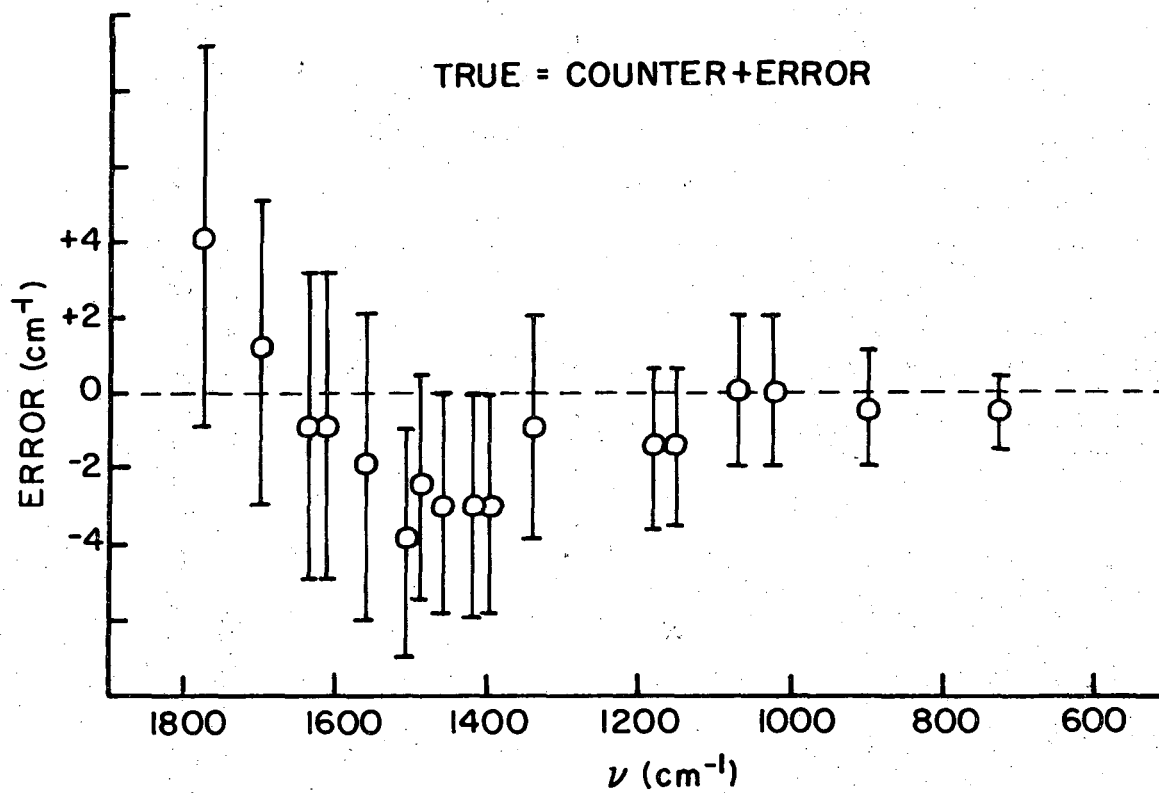
Fig. 5. Accuracy of monochromator counter readings.

F. Characterization of the Pressure Scale

Using "Drickamer" type cells, Wiederkehr and Drickamer in their work on cyanide solutions,[58] and Nicol et al. in their studies of Quartz,[59] inorganic cyanides,[60] and carbonates[61] establish that the relationship between applied load and pressure is linear.[*]

The primary calibration of the cell depends upon the decrease in intensity of transmitted light through a sample undergoing a phase transition. Light scattering generally increases at the onset of a transition. A crystalline sample of KBr was studied as a function of applied load. The frequency is maintained at 2,100 cm^{-1} and transmittance is measured as the load increases. Figure 6 shows the unmistakable phase transition. The pressure at the transition from a NaCl to a CsCl structure was reported to be 18.1 kb by Bridgman.[62] Our calibration shows that the pressure on the sample is 0.784 of that calculated by dividing the applied load by the cross-sectional area of the WC piston. This is consistent with the work of Davies[63] on the pressure dependence of the absorption spectrum of nickel dimethylglyoxime.

In order to achieve some measure of consistency in infrared-high pressure studies, we duplicated the work of Wu[64] on single crystal polyethylene sheets (0.003 cm thickness, Marlex 6009, 95% single crystalline).[†]

---

[*] At least in new cells. As the cell becomes older, the sample chamber tends to enlarge. When this happens, the insert can be pressed out and replaced or, what is far easier, larger diameter WC discs, machined to fit the sample chamber, can be used. In one year of use, the sample chamber diameter increased by only about 0.1%.

[†] Note that C. K. Wu defined the pressure on his samples as the ratio of applied load to piston area. We show that, while Wu's data are extremely precise, all of his pressures must be multiplied by about 0.78 to be correct.
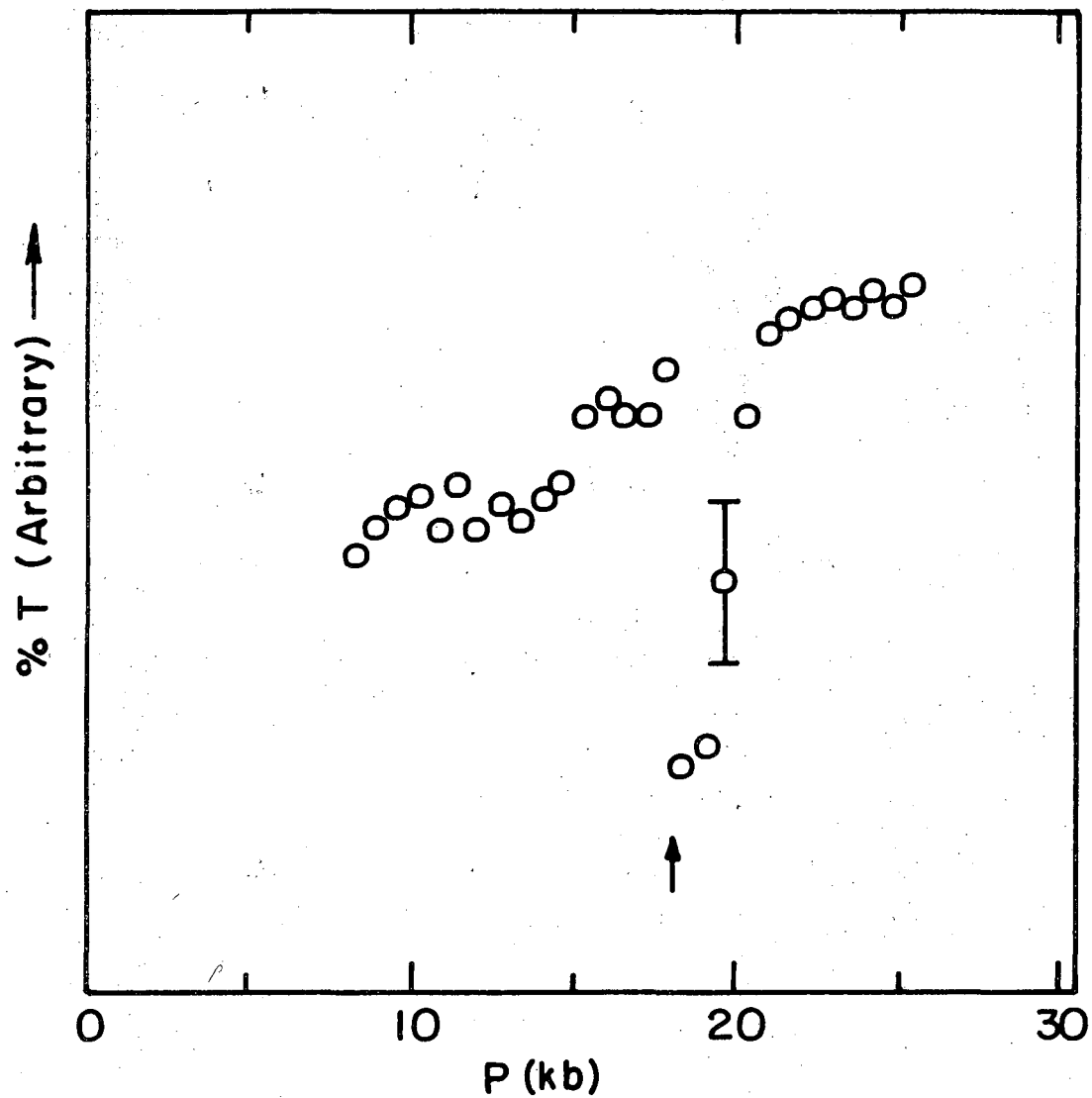
XBL 748-7089

Fig. 6. Intensity of transmitted 2,100 cm^{-1} radiation through solid KBr.

The shift of the 730 cm^{-1} absorption is seen to be linear with applied load (Fig. 7). Also, we consider the pressure across the sample to be uniform for the following reason. The measured shift of the 730 cm^{-1} band, which is narrow and symmetrical, is not only linear and large, but there is no broadening throughout the pressure range investigated. We also show a plot of the CN$^-$ stretching frequency vs pressure in crystalline NaCN (Fig. 8). These two plots provide a secondary standardization of our pressure scale.
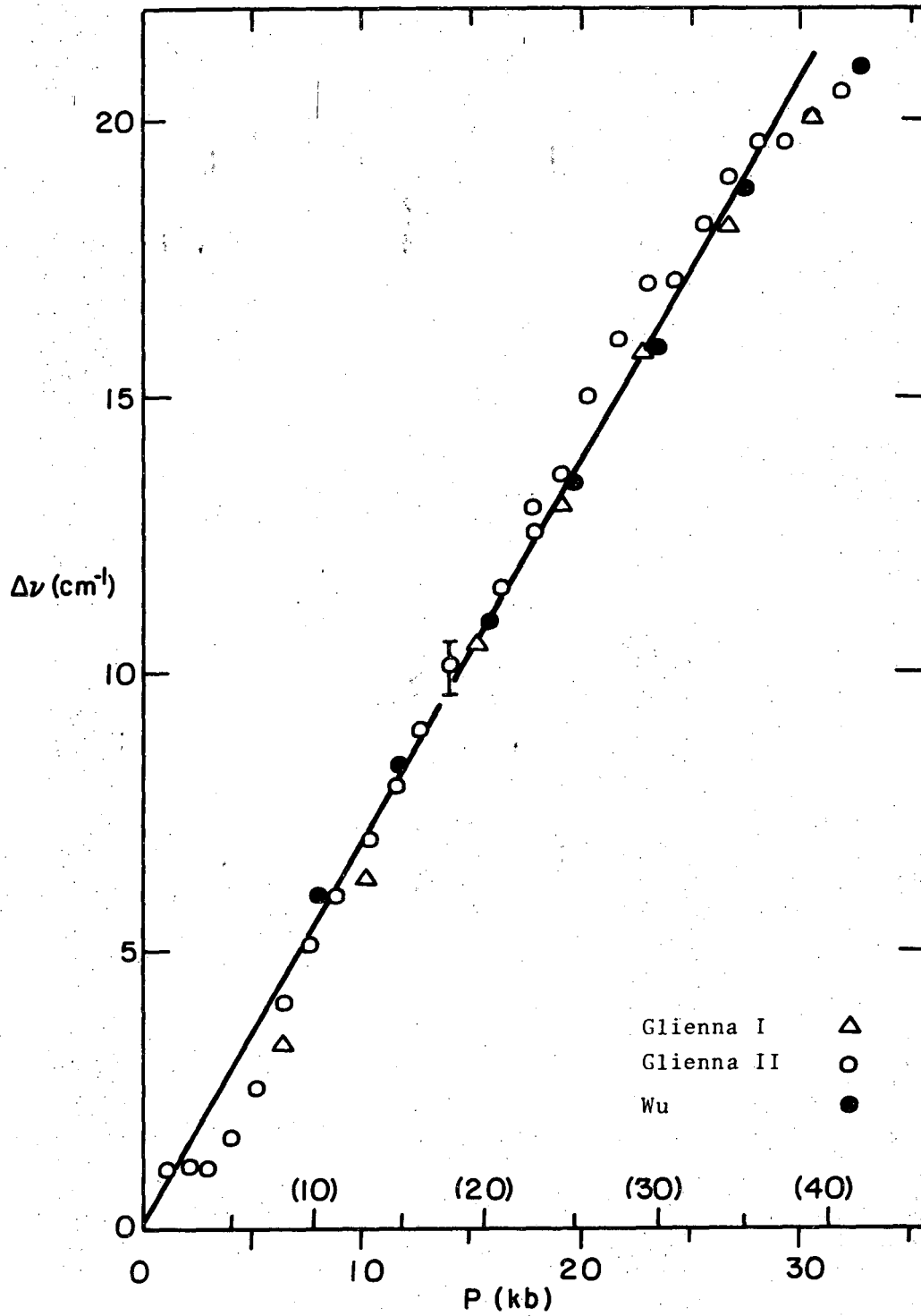
Fig. 7. Frequency of "730 cm^{-1}" absorption of polyethylene from one atmosphere presure to 35 kb. Numbers in parenthesis represent Wu's pressure scale.
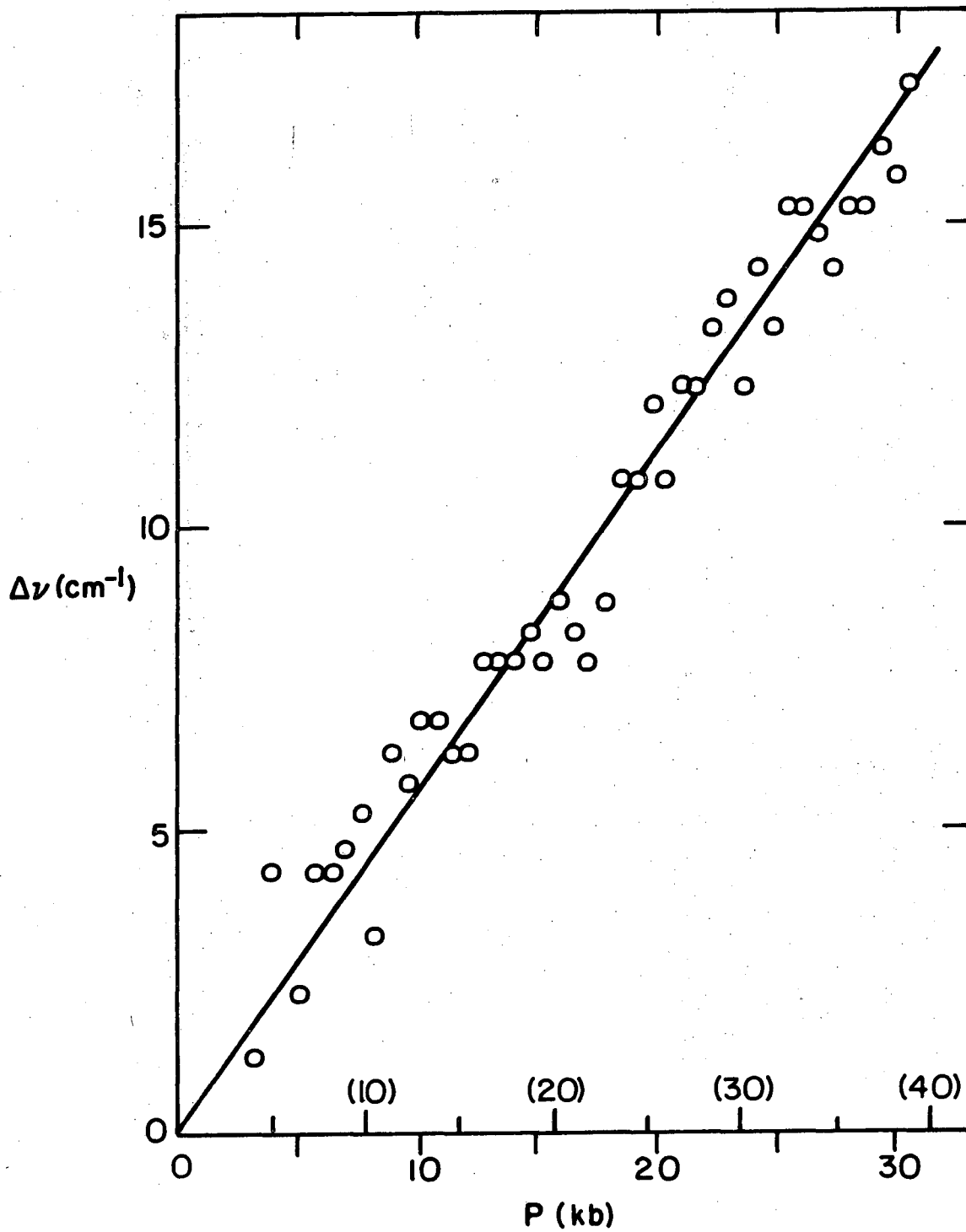
XBL 748 - 7079

Fig. 8. Frequency of CN⁻ stretching vibration in solid NaCN
from one atmosphere pressure to 30 kb.

XBL 748-7078

IV. RESULTS AND DISCUSSION

A. Infrared Spectra of TCB and DCB at High Pressure

TCB and DCB are planar molecules with approximately D_{2h} symmetry.
This discounts isotope effects which affect and complicate the vibra-
tional spectra of the solids in the following manner. Naturally oc-
curring chlorine atoms are approximately 75% Cl^{35} and 25% Cl^{37}. This
means that a group of TCB molecules synthesized from natural chlorine
will consist of the following species:

$$31.6\% \quad 4Cl^{35}$$
$$42.2\% \quad 3Cl^{35}, \; 1Cl^{37}$$
$$21.1\% \quad 2Cl^{35}, \; 2Cl^{37}$$
$$4.7\% \quad 1Cl^{35}, \; 3Cl^{37}$$
$$0.4\% \quad 4Cl^{37} \quad .$$

These should be distributed randomly within a TCB lattice. Clearly,
each vibrational band of TCB will consist of superpositions of fre-
quencies due to the presence of the above molecules. Therefore, both
intermolecular and isotope effects will always be present. As a result,
the absorptions in the solid tend to be broad and asymmetric with many
small maxima. This makes the determination of the absorption frequency,
if it is even permissible to speak of such a frequency, difficult and
arbitrary. We believe that measurements of frequency shifts with pres-
sure are more meaningful than the stated frequencies themselves. The
shifts measure only the change in frequency of some identifiable part
of an absorption band, not necessarily a peak.

At room temperature and pressure TCB crystallizes in a β-phase which is monoclinic space group C_{2h}^5 (P2$_{1/a}$). The a-axis makes an angle β = 103.5° with the c-axis, and the unit cell dimensions are a = 9.73, b = 10.63 and c = 3.86 A.[65,66] Two molecules occupy the unit cell at the center and corner in the bc-plane. One molecule in the unit cell transforms into the other by reflection in the ac-plane and then translation along c by $\frac{1}{2}$c. DCB has the same crystal structure at room temperature and pressure with lattice constants a = 14.83, b = 5.88, c = 4.10 A, β = 112.5°.[67] TCB also exists in a triclinic α-phase below 188 K. [68]

Infrared absorption spectra of TCB and DCB have been studied by Saeki,[69] Scherer,[70] Scherer and Evans,[71] and Stojiljhovic and Whiffen.[72] The spectra are well characterized in solution and in the solid state at atmospheric pressure. D'Alessio and Bonadeo[73] measured Raman scattering of TCB. Neutron scattering from TCB and DCB crystals was studied by Reynolds et al.[74]

We studied the infrared absorption spectra of solid TCB and DCB as functions of frequency and of pressure between 2000 and 750 cm^{-1} to 35 kb. We measured spectra of both single crystal and powdered reagent grade TCB and of powdered reagent DCB. The samples, which were usually about 0.005 cm thick, were studied with the high pressure infrared techniques described earlier. Results are shown in Tables IV and V. The symmetry assignments are after reference 71.

In TCB the absorptions at about 884, 1058, 1120, 1238, 1325 and 1443 cm^{-1} are the only fundamentals expected in this region. The bands near 1250 and 1478 cm^{-1} are combinations, the latter having high

Table IV. Fundamental frequencies of TCB as a function of pressure

Pressure (kb)	Frequency (cm^{-1})			
0	884	1058	1120	1238
2.5	884	1058	1120	---
5.1	883	1059	1120	1240
7.6	884	1059	1119	1242
10.2	884	1060	1121	1243
12.7	885	1060	1121	1245
15.2	886	1061	1123	1245
17.8	886	1063	1123	---
20.3	886	1063	1124	1248
22.9	887	1065	1126	1249
25.4	886	1065	1127	1252
27.9	887	1065	1126	1253
30.5	886	1067	1127	1254
Symmetry	B_{3u}	B_{1u}	B_{2u}	B_{2u}

Table IV.   (continued)

Pressure (kb)	Frequency (cm^{-1})		
0	1325	1443	*1478
2.5	1326	1444	.1478
5.1	1325	1443	1477
7.6	1326	1445	1478
10.2	1329	1447	1478
12.7	1333	1447	1478
15.2	1332	1448	1479
17.8	1333	1448	1477
20.3	1336	1448	1479
22.9	1336	1450	1480
25.4	1338	1450	1480
27.9	1340	1452	1481
30.5	1341	1452	1479
Symmetry	B_{1u}	B_{2u}	B_{2u}(combination)

*Included as part of a Fermi Doublet with 1443 (B_{2u})

Table V.   Fundamental frequencies of DCB as a function of pressure

Pressure (kb)	Frequency (cm^{-1})			
0	817	955	1009	1083
2.5	819	957	1009	----
5.1	815	957	1011	1084
7.6	----	959	1011	1086
10.2	813	958	1012	1084
12.7	815	958	1012	1085
15.2	815	960	1011	1084
17.8	----	963	1014	1085
20.3	817	966	1015	1087
22.9	815	965	1015	1085
25.4	812	967	1018	1087
27.9	813	968	1017	1090
30.5	----	967	1017	1090
Symmetry	B_{3u}	A_u	B_{1u}	B_{1u}

Table V. (continued)

| Pressure (kb)	Frequency (cm^{-1})		
0	1100	1395	1477
2.5	1101	1395	1477
5.1	1101	1394	1477
7.6	1103	1396	1478
10.2	1104	1397	1479
12.7	1103	1397	1477
15.2	1106	1397	1479
17.8	1108	1398	1483
20.3	1108	1398	---
22.9	1108	1398	1480
25.4	1109	---	1484
27.9	1111	---	1482
30.5	1110	---	1484
Symmetry	B_{2u}	B_{2u}	B_{1u}

intensity, resulting from a resonance interaction (Fermi resonance) with the 1443 cm^{-1} fundamental.

Eight absorption bands due to fundamentals of DCB should lie between 2000 and 750 cm^{-1}. We were able to get good pressure data on only seven of them. Our plots of absorption frequency vs pressure for TCB and DCB are shown in Figs. 9 through 15. For each molecule, one absorption of each symmetry type is represented.

The plots show that for both TCB and DCB, all in-plane modes have a large positive shift of frequency as the solids are subjected to increasing pressure. That is, $\Delta\nu/\Delta P$ is positive and equal to at least 10 cm^{-1} in 30 kb for TCB and 6 cm^{-1} in the same pressure range for DCB. The behavior of the out-of-plane, B_{3u}, modes is different. While the B_{3u} absorption near 884 cm^{-1} for TCB has $\Delta\nu/\Delta p > 0$, its slope is only about one-third of the slope of the in-plane mode least affected by pressure. In DCB the out-of-plane mode near 815 cm^{-1} experiences a shift to _lower_ frequencies with increasing pressure. These results are quite significant and will be justified in terms of intermolecular dipolar coupling.

Table VI lists the measured absorption frequencies of TCB and DCB grouped according to symmetry properties. Pressure derivatives are included in the table.

In addition to the solid state studies, we measured the infrared spectra of solutions of TCB and DCB. Such solution spectra are important for two reasons. Firstly, the comparison of lineshapes in solution and in the solid state is critical in identifying crystal effects. Secondly, ν_S, the vibration frequency of a mode in an
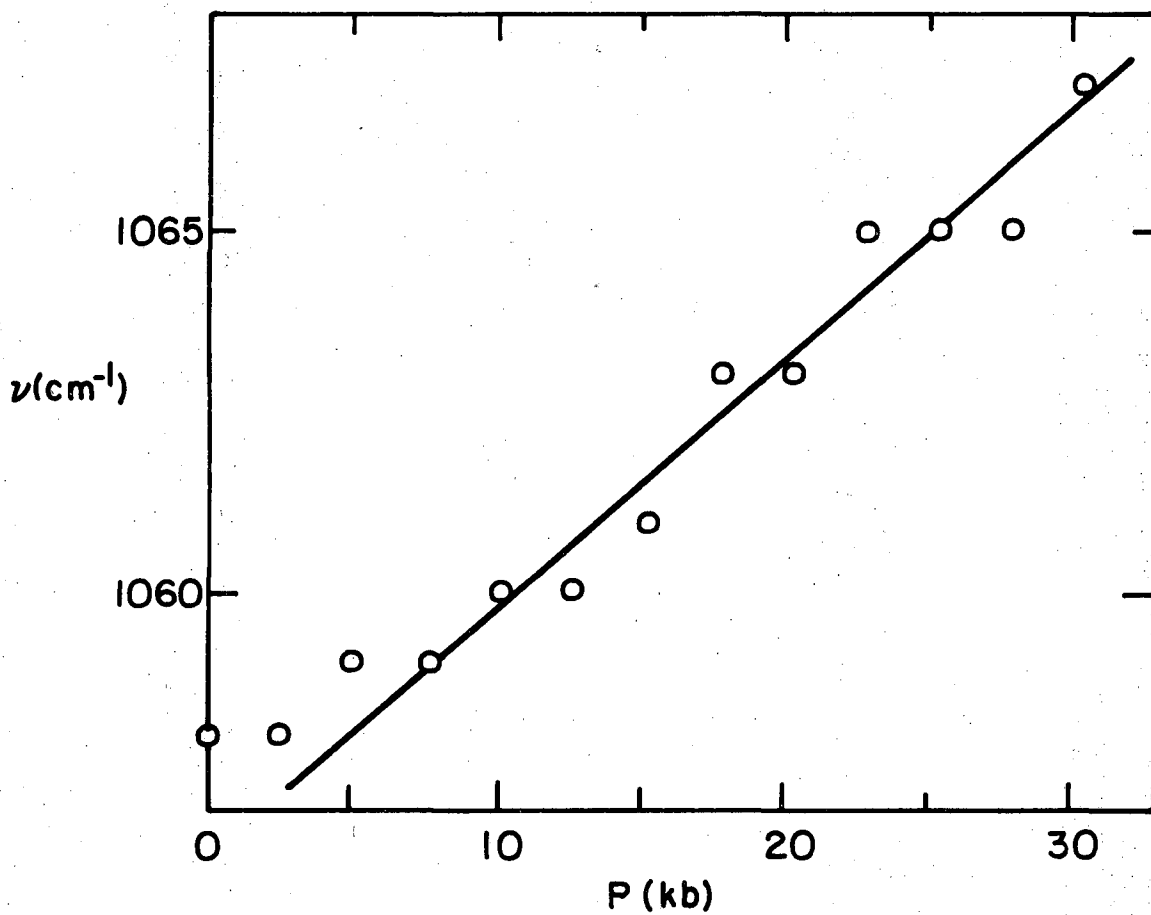
XBL 748-7085

Fig. 9. TCB, B_{1u} vibration.
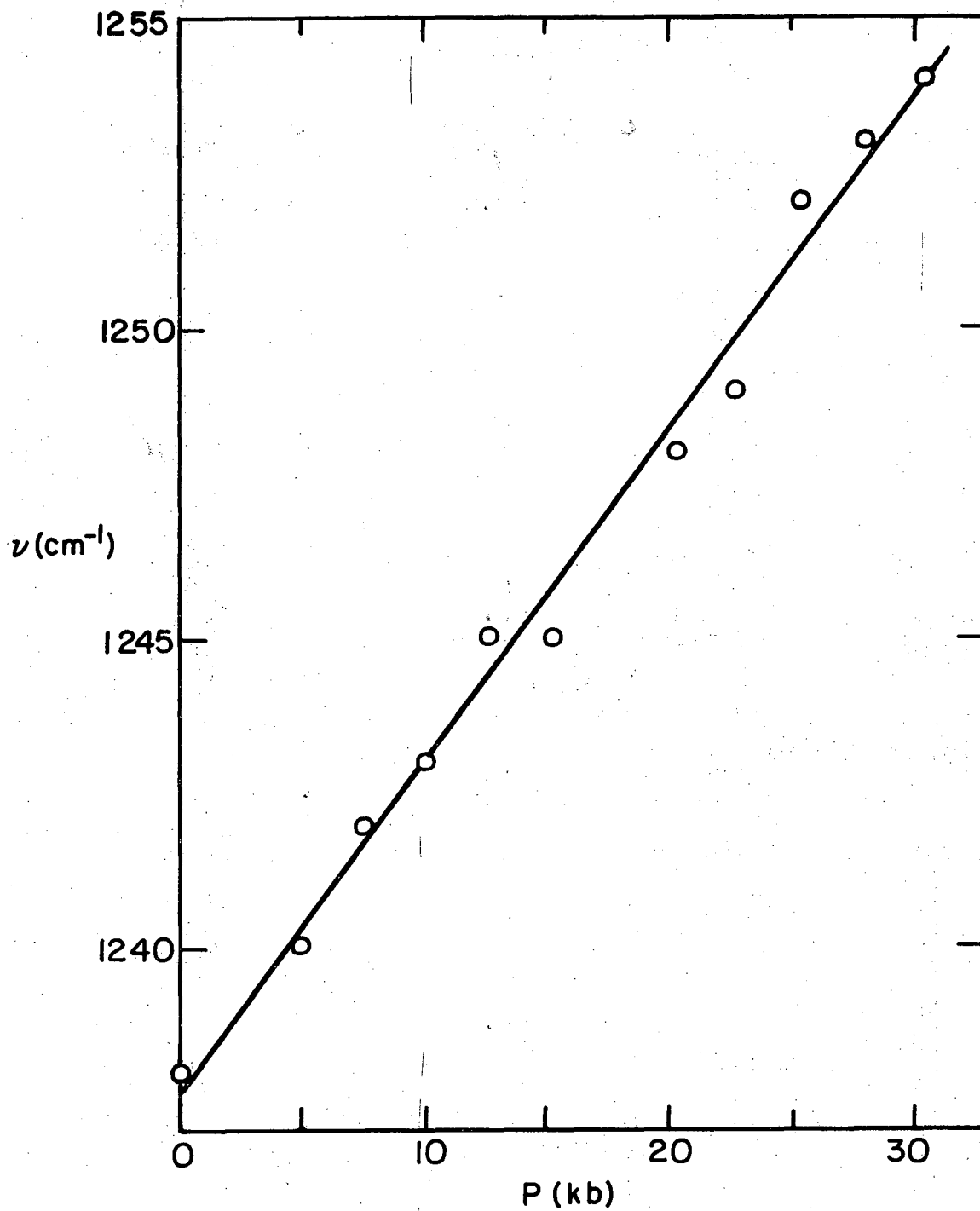
Fig. 10. TCB, B_{2u} vibration.

XBL 748-7086

XBL748-7084

Fig. 11. TCB, B$_{3u}$ vibration.
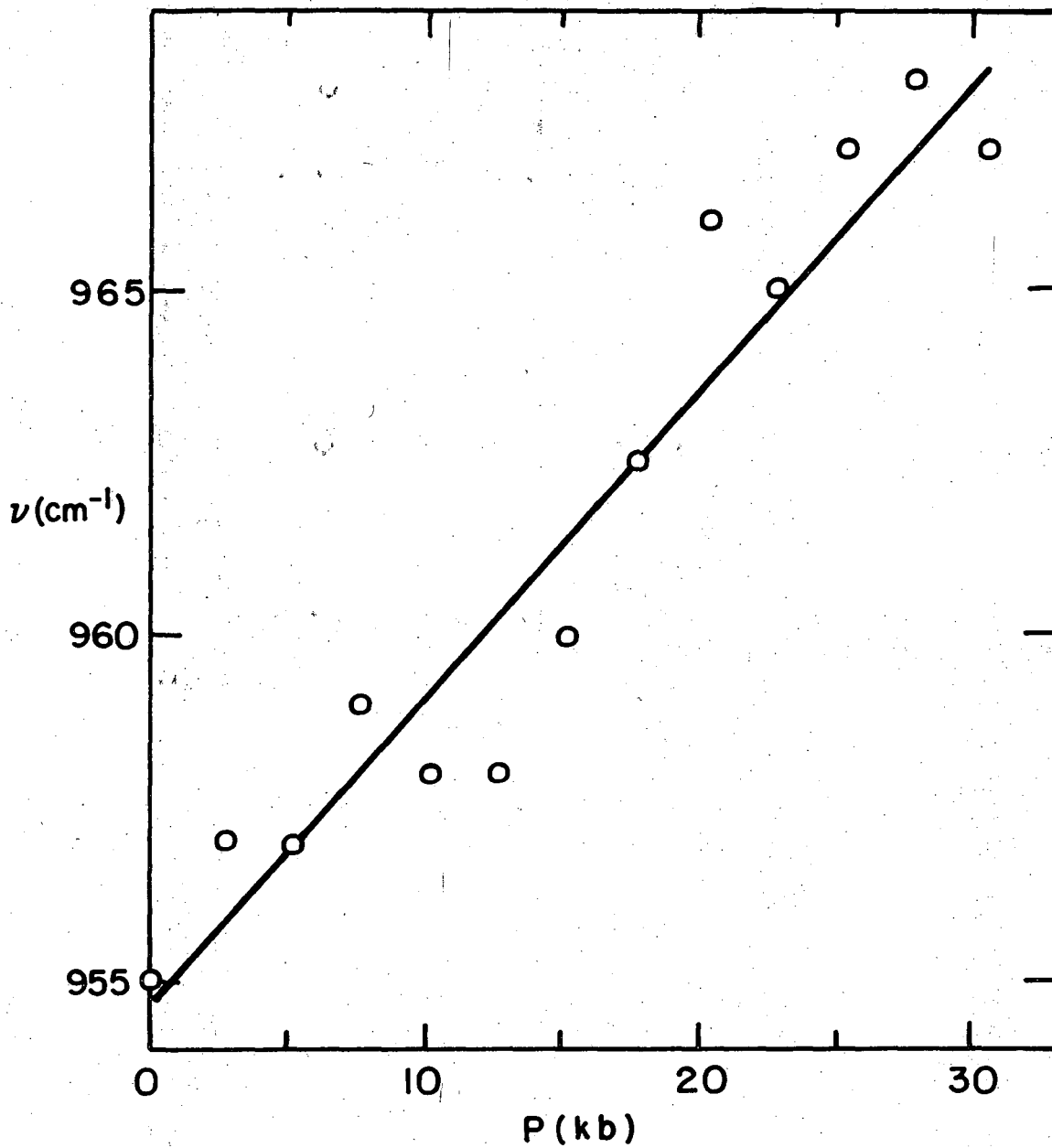
XBL 748-7081

Fig. 12. DCB, A_u vibration.
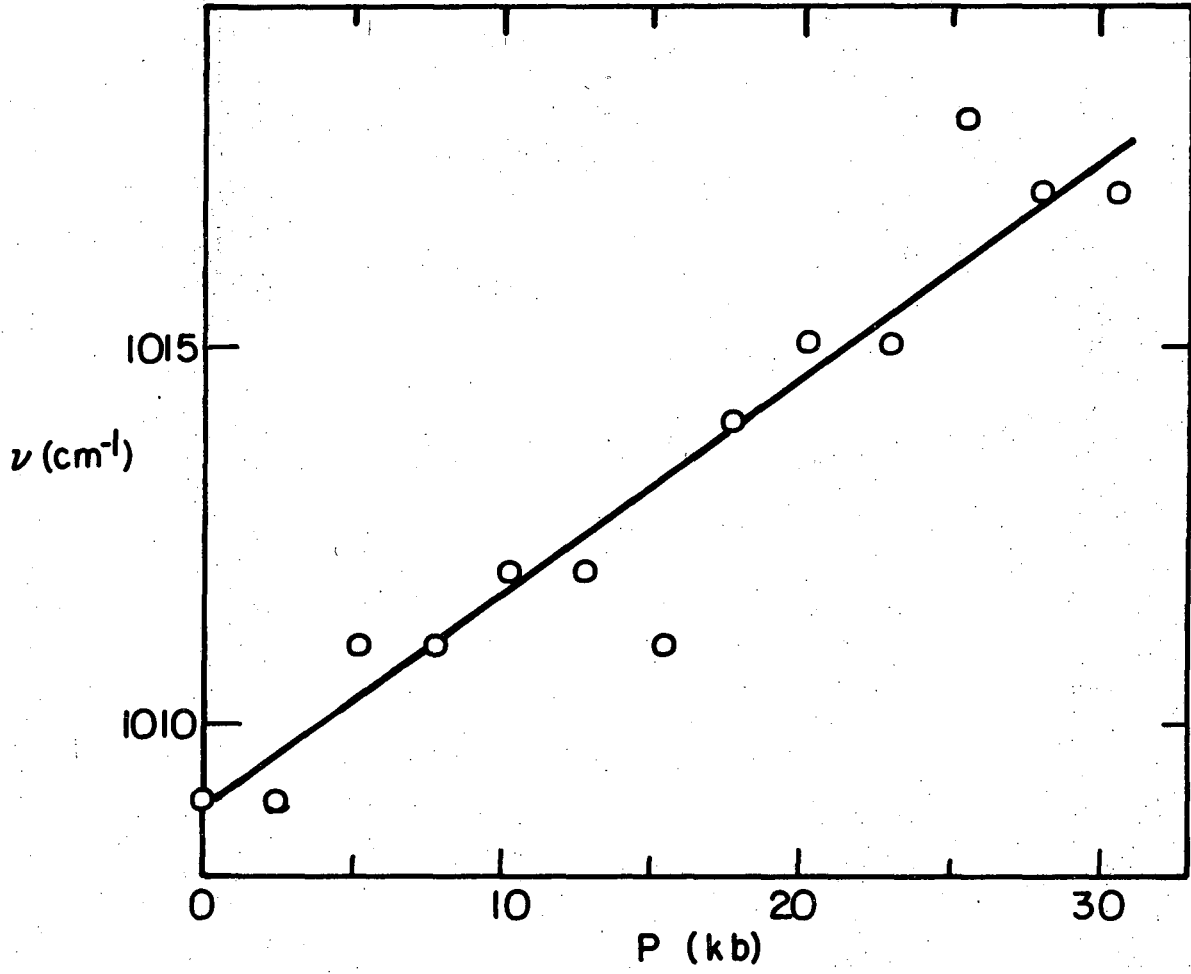
XBL748-7082

Fig. 13. DCB, B_{1u} vibration.
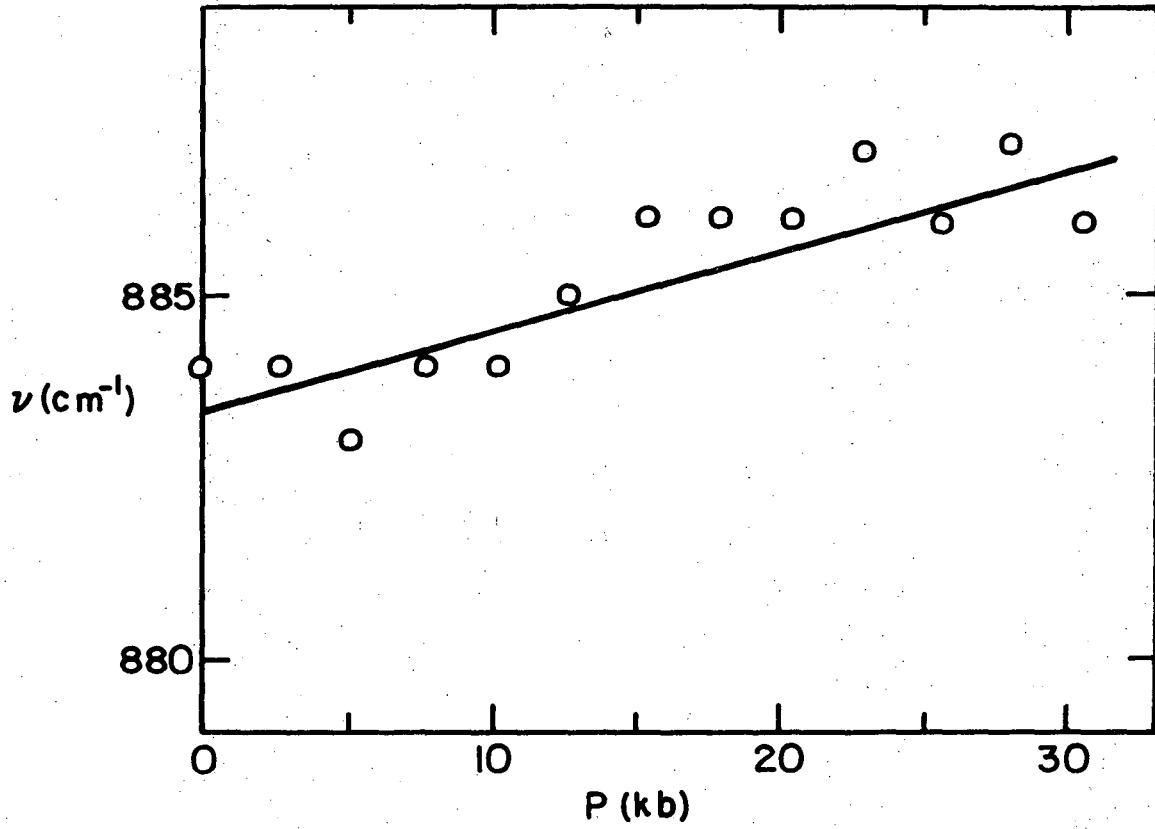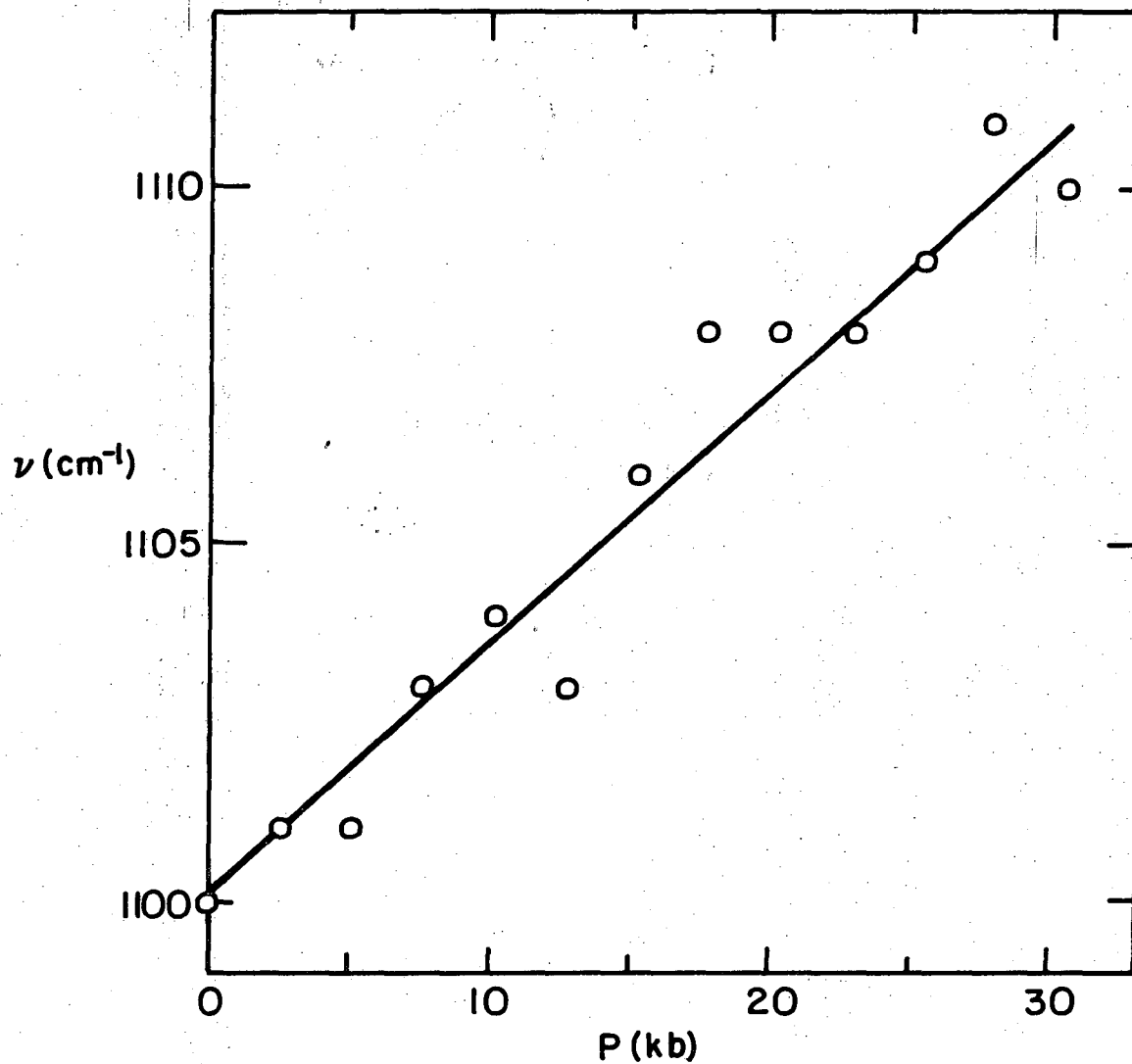
Fig. 14. DCB, B_{2u} vibration.
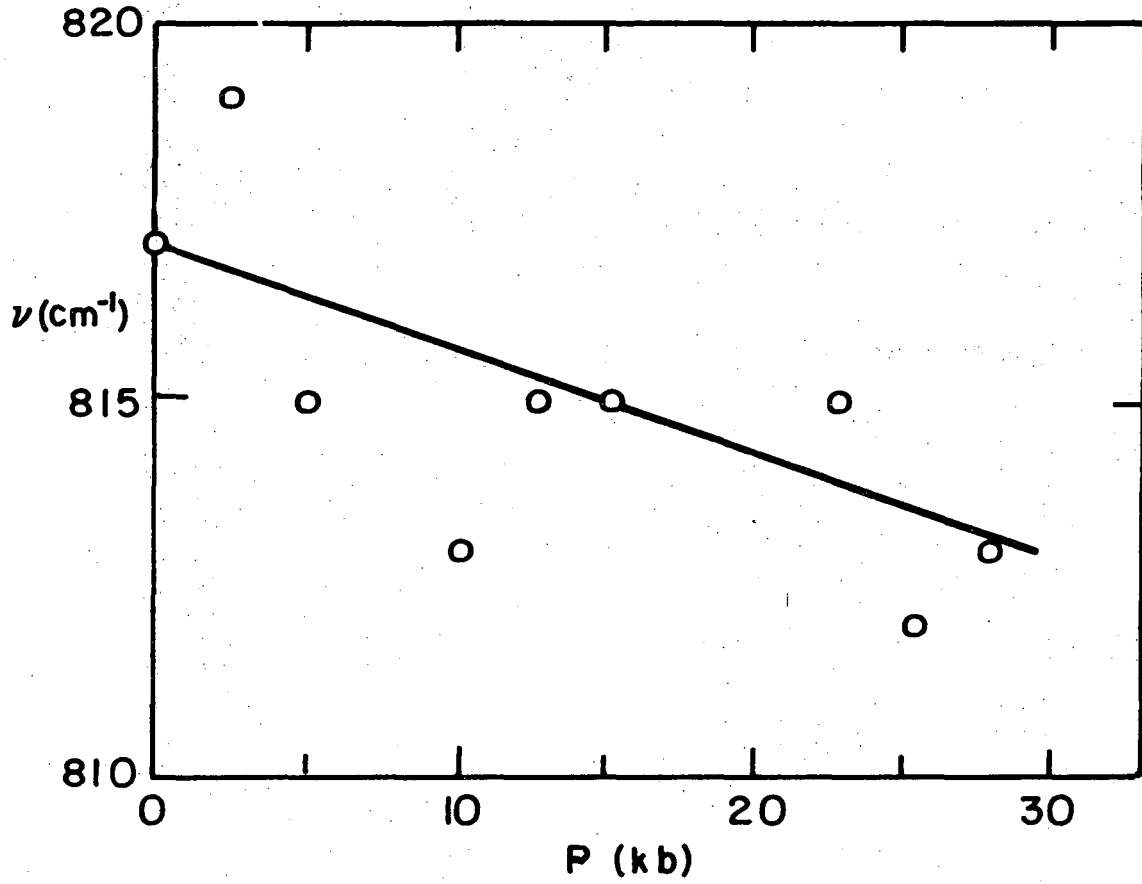
XBL 748-7083

XBL 748-7077

Fig. 15. DCB, B_{3u} vibration.

Table VI. Frequencies grouped by symmetry

	$\nu_o(cm^{-1})$	$\Delta\nu/\Delta P(cm^{-1}/kb)$	$\frac{1}{\nu_o}\Delta\nu/\Delta P(kb^{-1})$
TCB			
B_{1u}	1058	0.34	0.00033
	1326	0.58	0.00044
B_{2u}	1119	0.32	0.00029
	1238	0.53	0.00043
	1442	0.32	0.00022
B_{3u}	883	0.11	0.00012
DCB			
A_u	955	0.43	0.00045
B_{1u}	1009	0.28	0.00028
	1083	0.23	0.00022
	1476	0.28	0.00019
B_{2u}	1100	0.35	0.00032
	1394	0.18	0.00013
B_{3u}	814	-0.14	-0.00017

isolated molecule, enters into the formulas for calculating the effective dipole perturbation (Eqs. 3 and 4).

The values of the frequencies in solution for the six normal modes of TCB studied are 879, 1119, 1062, 1229, 1326 and 1447 cm^{-1}. In solutions of DCB the fundamentals of interest occur at 817, 951, 1013, 1087, 1104, 1393 and 1475 cm^{-1}. Spectra were studied using benzene and chloroform as solvents, and frequencies are reported only for those modes for which we have pressure data in the solid state.

B. Dipole Lattice Sums

Calculation of the transition dipole-transition dipole sums Γ_{11} and Γ_{12} in Eqs. (3) and (4) is complicated by the fact that such sums are only conditionally convergent in three dimensions.[75] Hexter in 1962[76] used a general procedure due originally to Nijboer and de Wette[77] to evaluate lattice sums in some cubic and tetragonal crystals. He had moderate success in explaining shifts of vibrational frequencies which occur upon condensation of molecules into the solid state. Many other authors have worked on dipole lattice sum calculations with hopes of explaining vibrational spectra of molecular and ionic solids. The work is typified by that of Decius et al.[78] There is less of a problem in evaluating the interaction lattice sums in one and two dimensions because the sums are convergent.

This is illustrated as follows: Consider a uniform, continuous distribution of dipoles surrounding a central dipole. In one dimension the number of dipoles contributing to the summation will increase by a small amount dN as we increase the distance from the central dipole by

dR. In two dimensions dN increases as RdR. The interaction decreases as R^3 so in one and two dimensions, the energy of interaction should be proportional to, respectively,

$$\int \frac{dR}{R^3} \quad \text{and} \quad \int \frac{RdR}{R^3}$$

which both converge rapidly.

As mentioned earlier, in their normal crystal structures, TCB has one lattice constant at least 2.5 times shorter than either of the other two, and DCB has one lattice constant at least 2.5 times longer' than the other two. These facts led us to believe that one and two dimensional models might be used in calculating dipole-dipole lattice sums for TCB and DCB respectively, thereby circumventing the problem of nonconvergence of such sums in three dimensions. Thus, in TCB we assume that interactions will occur primarily along the a-crystal direction, and in DCB interactions will occur among molecules lying mainly in the b-c crystal plane.

Along the a-axis in crystalline TCB all molecules belong to the same translationally equivalent set. In crystalline DCB the bc-plane, likewise, contains only translationally equivalent molecules. Therefore, in calculating the dipole sums in Eqs. (3) and (4), all terms Γ_{12} are identically zero in our one and two dimensional approximations (Γ_{12} calculates the interaction of a central molecule only with translationally inequivalent neighbors).

We determined dipole unit vectors along the three principal, molecular, inertial axes for TCB and DCB assuming D_{2h} symmetry. Tables

VII and VIII give the transformations of these vectors into lattice-based coordinates. For example, in DCB,

$$E_Y = 0.5293x + 0.6453y + 0.5507z$$

and

$$E_Y = 0.5293x - 0.6453y + 0.5507z$$

for any two translationally inequivalent DCB molecules.

We set up separate lattices for TCB and DCB using the previously stated values of lattice constants and included angles. A central lattice point is selected as origin. Dipoles, E_X, E_Y and E_Z are placed at each point on the lattice and are oriented to maintain the space group symmetry. They represent and have the same direction as the transition dipoles E_X, E_Y and E_Z of TCB and DCB. We then (i) calculate the angular factors (dot products) in Eq. (1) for each dipole with the central dipole, (ii) divide each factor by the cube of the distance separating the dipoles and (iii) sum in one dimension for TCB and in two dimensions for DCB. There is, of course, no problem with convergence (in this case an answer within 10% of the true value is adequate).

The lattice constants a, b, and c are reduced by fractions of their values at atmospheric pressure and the angular factors and sums are re-evaluated. In this way the unit cell is gradually reduced to about 90% of its original volume, with dipole lattice sums calculated for several unit cell volumes. Table IX lists results of the dipole sum calculations for the one and two dimensional models at two different unit cell volumes.

Included in the same table are our results of the same calculations done for three dimensional lattices of TCB and DCB. These sums

Table VII. Transformation from lattice-based coordinates to molecule-based coordinates for TCB. (Right-handed coordinate axes, y parallel to b, z parallel to c, x perpendicular to the plane formed by b and c)

"Molecule A" of bimolecular unit cell, β-phase.

$$
\begin{pmatrix} X \\ Y \\ Z \end{pmatrix} = \begin{pmatrix} -0.5129 & 0.2134 & 0.8292 \\ 0.6886 & 0.6800 & 0.2153 \\ 0.5484 & -0.6626 & 0.5100 \end{pmatrix} \begin{pmatrix} x \\ y \\ z \end{pmatrix}
$$

"Molecule B" is related to "molecule A" through the transformation of (x, y, z) by

$$
\begin{pmatrix} 1 & 0 & 0 \\ 0 & -1 & 0 \\ 0 & 0 & 1 \end{pmatrix}
$$

followed by operation with "molecule A" transformation. (X, Y, Z are molecule-based and x, y, z are lattice-based)
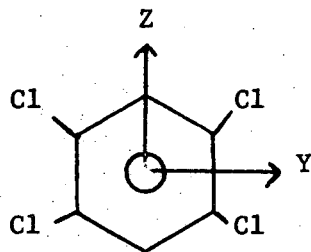
Table VIII. Transformation from lattice-based coordinates to molecule-based coordinates for DCB. (Right-handed coordinate axes, y parallel to b, z parallel to c, x perpendicular to the plane formed by b and c)

"Molecule A" of bimolecular unit cell

$$\begin{pmatrix} X \\ Y \\ Z \end{pmatrix} = \begin{pmatrix} -0.3239 & -0.4463 & 0.8343 \\ 0.5293 & 0.6453 & 0.5507 \\ -0.7890 & 0.6130 & 0.0401 \end{pmatrix} \begin{pmatrix} x \\ y \\ z \end{pmatrix}$$

"Molecule B" is related to "molecule A" through the transformation of (x, y, z) by

$$\begin{pmatrix} 1 & 0 & 0 \\ 0 & -1 & 0 \\ 0 & 0 & 1 \end{pmatrix}$$

followed by operation with "molecule A" transformation. (X, Y, Z are molecule-based and x, y, z are lattice-based)
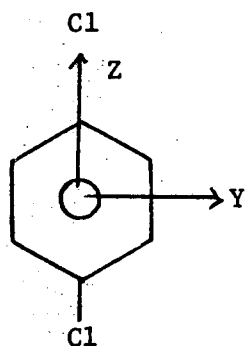
Table IX. Dipole lattice sums

		$E_X(A^{-3})$	$E_Y(A^{-3})$	$E_Z(A^{-3})$
TCB				
(one dimension)				
Γ_{11}/μ^2	V_o	−0.042	0.033	0.0087
	$0.94V_o$	−0.045	0.035	0.0092
(three dimensions)				
Γ_{11}/μ^2	V_o	−0.037	0.027	0.0093
	$0.94V_o$	−0.039	0.029	0.0099
Γ_{12}/μ^2	V_o	0.010	0.0062	0.012
	$0.94V_o$	0.011	0.0065	0.013
DCB				
(two dimensions)				
Γ_{11}/μ^2	V_o	−0.032	−0.0010	0.034
	$0.94V_o$	−0.035	−0.0011	0.036
(three dimensions)				
Γ_{11}/μ^2	V_o	−0.033	0.0026	0.032(0)
	$0.94V_o$	−0.035	0.0028	0.032(1)
Γ_{12}/μ^2	V_o	0.0039	−0.0031	−0.025
	$0.94V_o$	0.0042	−0.0039	−0.026

consist of terms for the interaction of a central molecule (dipole) with 431 of its neighbors (215 translationally equivalent and 216 translationally inequivalent neighbors). Each three dimensional lattice has the overall shape of the monoclinic unit cell.

What we were trying to do by evaluating the lattice sums at different volumes was to investigate the effects of pressure on the sum. We had no idea, a priori, what the detailed effects of hydrostatic compression would be on the individual lattice constants.* Therefore, we were forced to make the assumption that the effect of subjecting the solid to a hydrostatic pressure is a uniform fractional reduction of each lattice constant. This is essentially the same as assuming identical linear compressibilities ($\doteq \frac{1}{L_o} \frac{\Delta L}{\Delta P}$) along each crystal axis. We wanted to correlate qualitatively the pressure effects on the dipole sums with the observed pressure dependence of the infrared spectra.

Notice from Table IX that the lattice sums in one dimension for TCB and in two dimensions for DCB closely match their three dimensional analogues. This is true in all but one case. For B_{2u} vibrations (E_Y) of DCB, the lattice sums are negative at both $V = V_o$ and $V = 0.94V_o$ in the two dimensional case. The corresponding sums in three dimensions are both positive. However, we do not believe this to be serious because the sums are very small. In fact, they are an order of magnitude less than the lattice sums calculated for $B_{1u}(E_Z)$ and $B_{3u}(E_X)$ in DCB. And inclusion or elimination of a few more terms in the evaluation

---

*Linear compressibility data on organic molecules is almost totally lacking. However, see Bridgman.[79]

of the three dimensional sum for E_γ could easily bring two and three dimensional values into agreement. At any unit cell volume

$$\nu \approx \nu_S \left(1 + \frac{\Gamma_{11}}{8\pi^2 c^2 \nu_S^2} \right)$$

for TCB (one dimensional model) or DCB (two dimensional model). ν, the vibrational frequency in the solid, is displaced from ν_S, the isolated molecule frequency by

$$\frac{\Gamma_{11}}{8\pi^2 c^2 \nu_S^2} \quad .$$

The value of ν/ν_S at any volume depends directly on Γ_{11}. Using our lattice sum calculations on TCB and DCB, we calculated ν/ν_S vs unit cell volume for vibrations of symmetries B_{1u}, B_{2u}, and B_{3u}. The values are shown with dashed lines in Figs. 16 and 17. The vertical and horizontal scales are the same for all three types of vibrations. From these model calculations we expect decreases in frequencies of B_{3u} (out-of-plane) modes of both DCB and TCB upon compression. B_{1u} and B_{2u} modes of TCB and B_{1u} modes of DCB should increase in frequency and the frequencies of B_{2u} modes of DCB should decrease slightly with pressure.

In Table VI we grouped the absorption frequencies of TCB and DCB according to symmetry. Compare the pressure derivatives of frequency in this table with the volume behavior of ν/ν_S in Figs. 16 and 17 ($\nu_o \approx \nu_S$). There is qualitative agreement between theory and experiment for the in-plane vibrations of TCB, and for the B_{1u} and B_{3u} vibrations
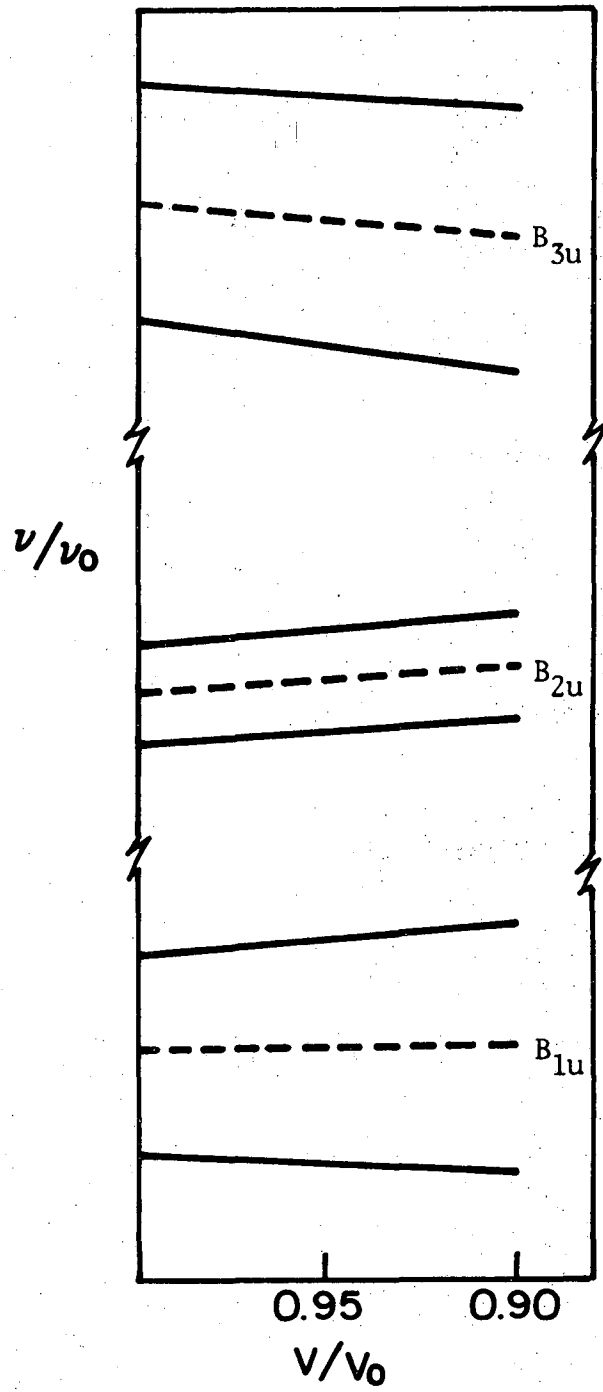
XBL 748-7090

Fig. 16. TCB.
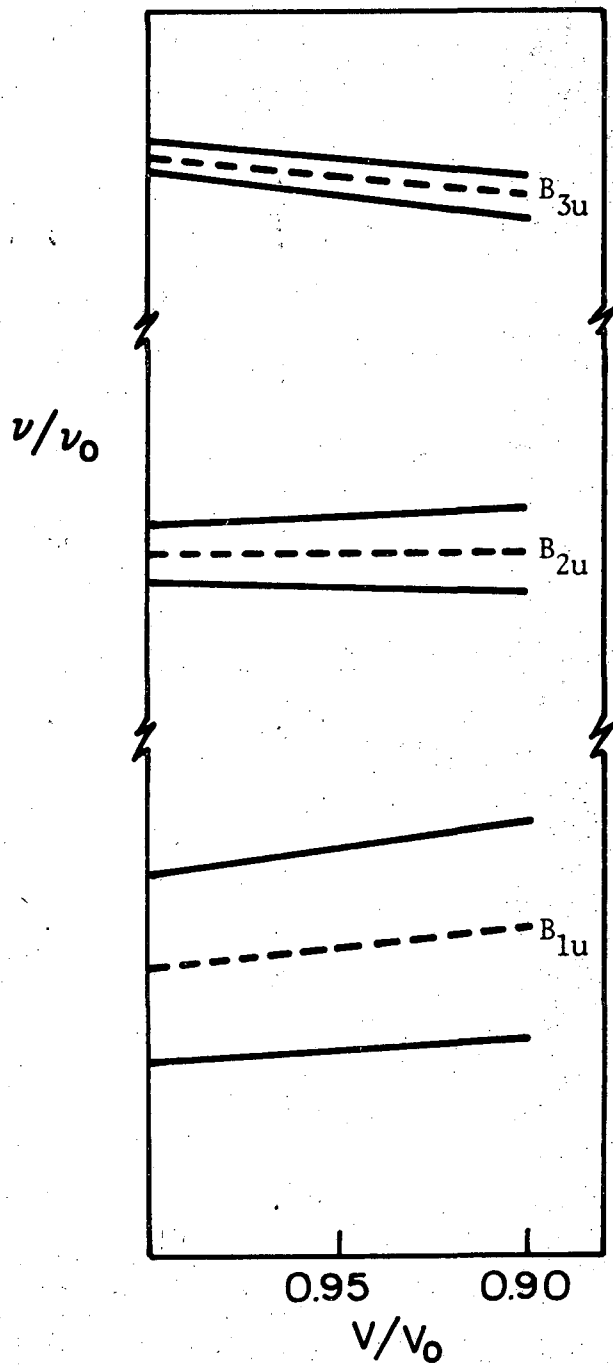
Fig. 17. DCB.

XBL748-7091

of TCB, and for the B_{1u} and B_{3u} vibrations of DCB. The calculated

and measured slopes are of opposite sign for the B_{3u} mode of TCB, and

for the B_{2u} mode of DCB. The B_{2u} disagreement presents no real problem.

Since the calculated slope of ν/ν_S vs volume is so small, slight

modifications in the method of evaluation or uncertainties in the crystal

structure could change the sign of the slope. In crystalline DCB,

the molecules deviate from planarity by a few percent.[80] Consequently,

by confining (as we have) the three transition moments of DCB to

conform to D_{2h} symmetry, we have forced a constraint upon the system

which does not actually exist. For this reason alone, the very small

B_{2u} dipole lattice sums should not be taken to represent physical

reality. All we can say is that the pressure effects on B_{2u} modes of

DCB should be small.

We can also rationalize the disagreement between calculated and

observed behavior of the out-of-plane vibrations of TCB. While the

experimental slope of frequency vs pressure is positive, it is by far

the smallest in magnitude for any TCB vibration. It seems that the

negative perturbation term, Γ_{11}, indeed affects the B_{3u} vibration and

tends to lower the frequency upon compression. But clearly, the

transition dipole-transition dipole interaction is not an accurate

description of the actual perturbation of this out-of-plane mode.

This points out an important fact. As mentioned in the section

on Vibrational Exciton Theory, the expression for interaction of two

dipoles (or transition dipoles) is valid only when the dipoles are

separated by a large distance with respect to their size. The centers

of two neighboring, translationally equivalent, TCB molecules are

separated only by one lattice constant, c, less than 4A. The planes

of the nearest neighbors are nearly perpendicular to the line joining

their centers, and the transition dipole direction for B_{3u}, E_x, is

almost parallel to the line. Although all harmonic vibrations are

assumed to be of infinitesimal magnitude, it is questionable whether

a dipole-dipole term can satisfactorily be used to describe the

complicated interaction of two charge distributions (two TCB molecules

whose "diameters" are about 6A) separated by 4A. We have more confidence

in the dipole-dipole expression when the molecular motion is perpen-

dicular to the line of centers in TCB.

C. Fermi Resonance in TCB

As stated previously, we see a strong doublet near 1450 cm^{-1} in

the infrared spectra of crystalline TCB. Also in both solution and

solid state spectra of TCB, Scherer and Evans[81] resolve two strong

bands near 1450 cm^{-1}. Their normal coordinate calculations identify

the absorptions as the two components of a Fermi doublet with a B_{2u}

fundamental near 1445 cm^{-1} and a B_{2u} combination band at 1478 cm^{-1}.

In the simple harmonic oscillator theory all overtone and combination

bands are disallowed under an electric dipole transition. But in

actual practice the appearance of these bands is due to either an-

harmonicity in the molecular motion or to terms higher than linear in

the expansion of the molecular dipole moment in normal coordinates.

Mechanical anharmonicity is usually more important and more easily

rationalized. We shall assume that this is the cause of the appearance

of the combination in this case.

Consider a two state system with the states well separated in energy and of the same symmetry. As their energy separation decreases, the two states interact such that each state (independent when well-separated) now contains admixtures of the two original states.

If the independent states are v_1 and v_2, the perturbed energy levels of the system are obtained by diagonalizing the matrix

$$\begin{pmatrix} E_1 & E_{12} \\ E_{12} & E_2 \end{pmatrix}$$

The two eigenvalues are

$$\lambda = E_1 + E_2 \pm \frac{1}{2} \delta \ ,$$

and

$$\delta = [(E_1 - E_2)^2 + 4E_{12}^2]^{1/2} \tag{8}$$

is the observed separation of the two states and $E_1 - E_2$ is the separation of the unperturbed levels.

The perturbed states are then

$$v_1' = av_1 - bv_2 \tag{9}$$

$$v_2' = bv_1 + av_2 \tag{10}$$

$$a = \left[\frac{\delta + (E_1 - E_2)}{2\delta} \right]^{1/2} \quad ; \quad b = \left[\frac{\delta - (E_1 - E_2)}{2\delta} \right]^{1/2}$$

The matrix elements E_1, E_2, and E_{12} are similar to those discussed earlier in the section on vibrational exciton theory, but here E_1 is not necessarily equal to E_2.
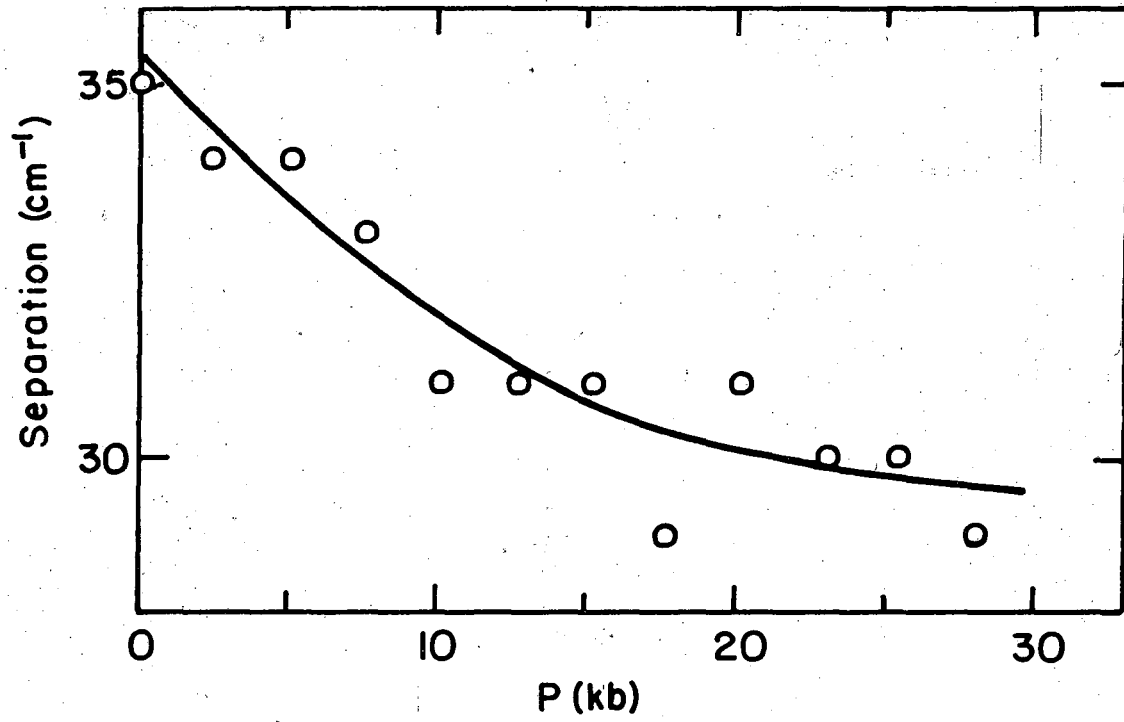
Fig. 18. Separation of Fermi resonance components near 1450 cm^{-1} in TCB.

Now, say that v_1 is the unperturbed upper state of a fundamental and v_2 is the upper state of a combination. A situation might exist where E_1 is less than E_2 at atmospheric pressure and E_1 greater than E_2 at high pressure (i.e., $\Delta E_1/\Delta P > \Delta E_2/\Delta P$). This appears to be what is happening with the Fermi doublet of TCB near 1450 cm^{-1}. (See Fig. 18)

From the observed energy level separations at various pressures we can calculate the unperturbed eigenvalues and the coefficients of mixing in Eqs. (8) and (9) provided that the off-diagonal element E_{12} is independent of pressure.* At a pressure of about 35 kb the separation of the two levels appears to be at a minimum ($\delta = 29.3$, $E_1 = E_2$). At higher pressures the separation should increase. We calculate from Eq. (8) $E_{12} = 14.6$ cm^{-1}. Table X shows $E_1 - E_2$, a, and b at various pressures for the two interacting states. Note that state v_1' consists mostly of v_1 at one atmosphere but contains mostly v_2 at high pressure.

---

*There is really no reason to believe that E_{12} should be much affected by pressure since it arises only from intramolecular interactions.

Table X. Unperturbed energy separations and coefficients of mixing for the B_{2u} resonance pair of crystalline TCB

| P (kb)	$E_1 - E_2$ (cm^{-1})	a	b
0	20.0	0.886	0.464
5	16.2	0.863	0.505
10	12.9	0.839	0.544
15	9.5	0.812	0.584
20	6.4	0.784	0.621
25	5.4	0.774	0.633
30	3.4	0.756	0.655
35	0	0.707	0.707
40 (calc)	3.4	0.655	0.756

D. Davydov Splitting in DCB

D'Alessio and Bonadeo in 1973 pointed out[82] that correlation field splitting (or Davydov splitting) is masked by isotopic effects in the solid chlorinated benzenes. We, however, are able to resolve an example of such a splitting in the infrared spectrum of DCB. The absorption near 1400 cm^{-1} is split into two components that are identifiable when the solid is subjected to a pressure of at least 15 kb. We know that this splitting is not due to isotopic effects for the following simple reason. The splitting increases from about 11 cm^{-1} to 15 cm^{-1} when the pressure on the sample is raised from 15 kb to 30 kb. In all the other absorptions of TCB and DCB, absorptions due to isotopic effects for any given vibration behave identically with pressure.

The absorption is redrawn at various pressures in Fig. 19. In Fig. 20 we show the splitting as a function of pressure.

From Eqs. (5) and (6), we know that a Davydov splitting, $\nu_1 - \nu_2$, is proportional to Γ_{12} at any pressure. In Table IX we calculated dipole lattice sums for B_{2u} modes of DCB (the vibration under discussion here is B_{2u}). Within our approximation, Γ_{12} increased by 25.8% as the unit cell volume decreased by 6%. Experimentally, $\Delta\nu/\Delta P = 0.24$ cm^{-1}/kb. From this data we can calculate a value for the (isothermal) compressibility of DCB,

$$- \frac{1}{V_o}\left(\frac{\Delta V}{\Delta P}\right)_T \quad .$$

Extrapolation to low pressures of the curve showing Davydov splitting vs pressure shows that $\Delta\nu$ (and therefore Γ_{12}) increases by 25.8% when the solid is compressed to 8.5 kb. Then
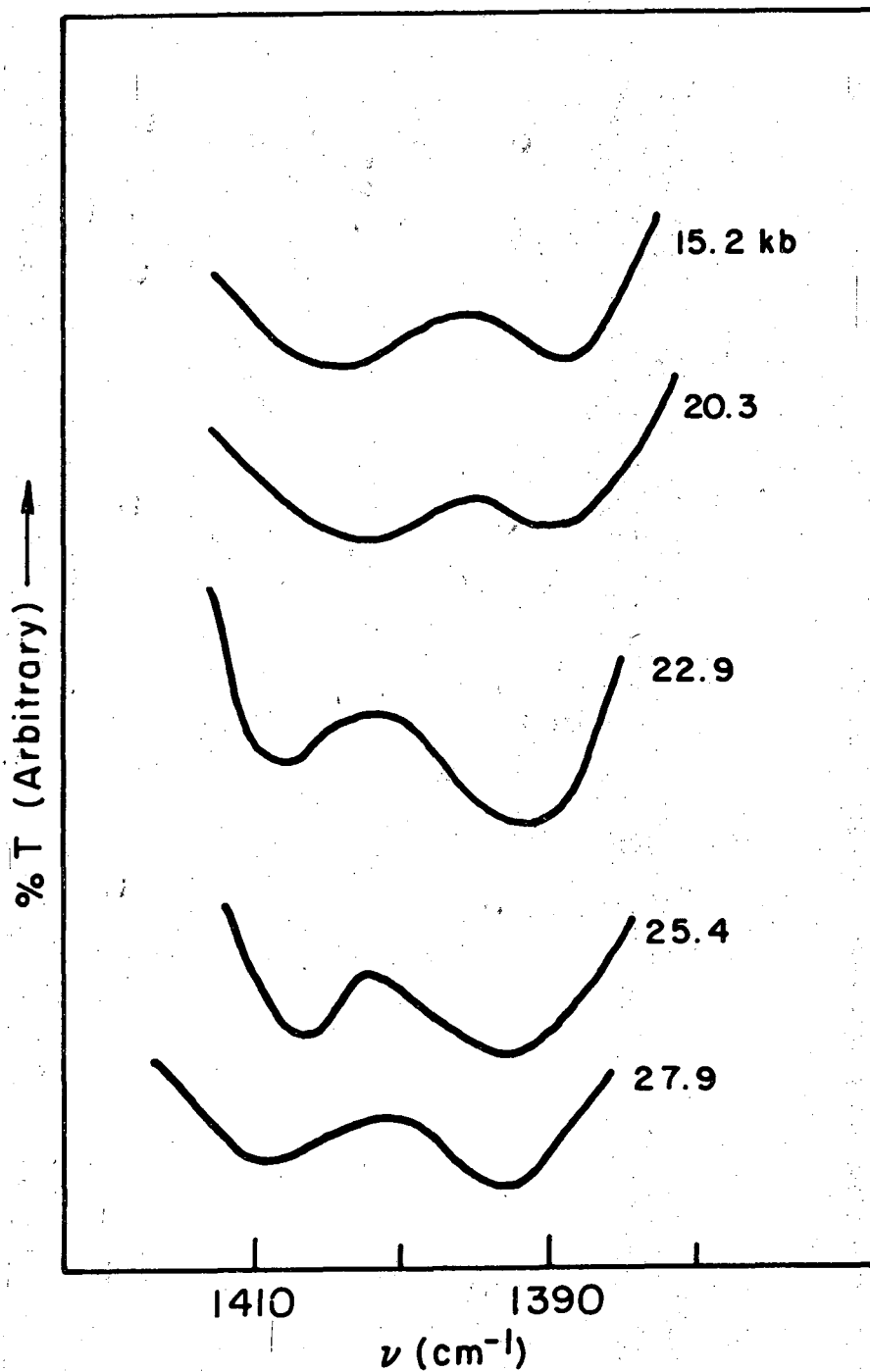
Fig. 19. Davydov splitting of 1394 cm^{-1} absorption of DCB at various pressures.
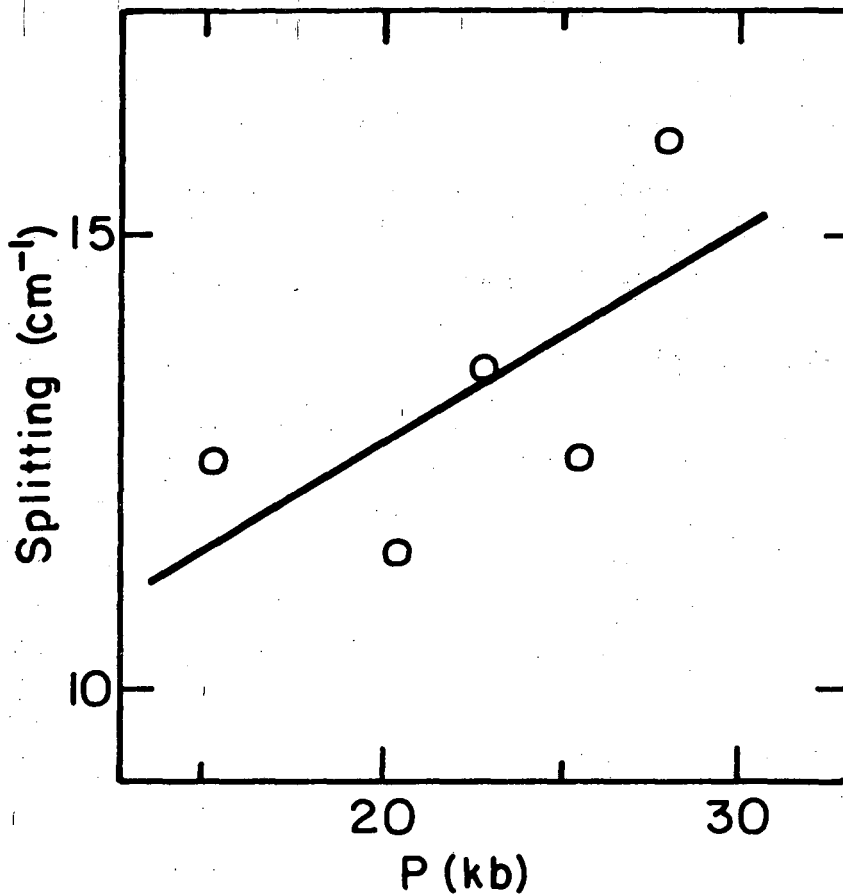
XBL748-7088

Fig. 20. Measured splitting of Davydov components. 1394 cm^{-1}, B_{2u} vibration of DCB.

$$\frac{1}{V_o} \quad \frac{0.06 \ V_o}{8500 \ \text{bar}} = 7 \times 10^{-6} \ \text{bar}^{-1}$$

Bridgman[83] measured the compressibilities of several organic

solids. We list the average compressibilities of naphthalene,

anthracene and benzophenone [all C_{2h}^5 (P2$_1$/a)] to 10 kb.

naphthalene $\quad\quad\quad 10.8 \times 10^{-6} \ \text{bar}^{-1}$

anthracene $\quad\quad\quad 8.4 \times 10^{-6} \ \text{bar}^{-1}$

benzophenone $\quad\quad 9.4 \times 10^{-6} \ \text{bar}^{-1}$

The agreement between these compressibilities and our calculated

compressibility of DCB is surprising!

E. Effect of High Pressure on the Out-of-plane Bending Modes

of Inorganic Carbonates. Dipolar Coupling

In 1954 Decius[84,85] tried to explain the complicated infrared

spectra of inorganic carbonates in the region of the $CO_3^=$ out-of-plane

bending mode, near 870 cm^{-1}. By simply adding a small correction term

to the vibrational force constant and by correcting for mass differ-

ences of $C^{12}O_3^=$ and $C^{13}O_3^=$, he was able to satisfactorily account for

the absorption band contours of C^{13} enriched carbonates. He later[86]

gave some theoretical justification to his calculations by proposing

that the correction term to the force constant for a carbonate ion in

a crystal was primarily due to coupling between the nearest neighbor

pairs of transition dipoles for the various normal modes.

For carbonates with the orthorhombic aragonite structure D_{2h}^{16} (Pcnm)

tetramolecular unit cell, the anions crystallize in parallel planes

with nearest neighbors displaced along the c-axis by $\frac{1}{2}c$. Lattice

constants for the alkaline earth carbonates are shown in Table XI.

The carbonate ion out-of-plane bending mode is particularly amenable

to investigation using the dipole-dipole theory because of the sim-

plicity of the interaction term. The angular factor in Eq. (1) for

nearest neighbor interactions reduces to -2, and we have

$$V = \frac{-2 \, \mu^2}{R^3} \ .$$

Granted that considering nearest neighbor interactions is

primitive, this approximation gives at least a qualitative feeling

for the coupling occurring in the crystal. Decius et al.,[88] themselves,

point out that results obtained by calculating complete dipole lattice

sums differ from those calculated using nearest neighbor interactions

by only 10 or 15% for the carbonates. This is certainly a figure

which can be tolerated considering that evaluating a dipole lattice

sum is difficult at best (even employing Ewald's method[89] as does

Decius), and totally unreliable at worst because of the shape-dependent

nature of the sum and usual neglect of coupling with lattice modes.

The frequency of the out-of-plane bend for a free carbonate ion

is given by

$$\nu^2 = \frac{1}{4\pi^2 c^2} \, (3\mu_c + \mu_o) \cdot F$$

in the harmonic approximation, where

$$C = 3 \times 10^{10} \text{ cm/sec}$$

F = force constant for the motion

μ_c and μ_o are the reduced masses of carbon and

oxygen, respectively.

Table XI. Lattice constants for alkaline earth carbonates

		a (A)	b (A)	c (A)
Argonite	(CaCO$_3$)	4.94	7.94	5.72
Strontianite	(SrCO$_3$)	5.12	8.41	6.03
Witherite	(BaCO$_3$)	5.31	8.90	6.43

(Orthorhombic, D_{2h}^{16} (Pcnm), tetramolecular unit cell,
see reference 87, p. 129)

		a (A)	α
Calcite	(CaCO$_3$)	6.75	46.12°

(Rhombohedral, D_{3d}^{6} (R$\bar{3}$c), bimolecular unit cell,
see reference 87, p. 127)

From the generally accepted value of the frequency, 879 cm^{-1},[90]
we calculate

$$F = 1.46 \times 10^5 \text{ dynes/cm} .$$

For absorption in naturally occurring carbonates with the aragonite
structure, the out-of-plane frequency should be very accurately ex-
pressed by[91]

$$\nu^2 = \frac{1}{4\pi^2 c^2} (3\mu_c + \mu_o)(F + 2F')$$

where

$$F' = -\frac{2\mu^2}{R^3}$$

in the nearest neighbor approximation with R = one-half lattice constant,
c. In calcite, R, the nearest neighbor distance of two carbonate ions,
is 4.98A.

We measured the frequencies of the out-of-plane bending modes of
carbonate ions in natural aragonite ($CaCO_3$), strontianite ($SrCO_3$),
witherite ($BaCO_3$) and calcite ($CaCO_3$) from atmospheric pressure to
over 30 kb. The samples were powdered and the experiments were per-
formed as discussed earlier. The results are listed in Table XII and
shown schematically in Fig. 21. Each band has a complicated shape, and
because of this and the lack of high light intensity in this region,
the frequencies are known with an uncertainty of 1.5 to 1.8 cm^{-1}.

Notice that the vibration frequency as a function of pressure for
the out-of-plane bends of the carbonate ions is strongly dependent on
the nature of the cation and on the crystal structure. The absorption
frequency in calcite is essentially constant to 30 kb. This agrees

Table XII. Frequencies of out-of-plane bends
of alkaline earth carbonates

P(kb)	Calcite	Aragonite	SrCO$_3$	BaCO$_3$
0	879	860	860	858
1.3	878	863	---	---
2.5	875	861	857	---
3.8	874	860	856	860
5.1	875	860	853	858
6.4	876	860	---	860
7.6	876	858	853	858
8.9	876	857	---	859
10.2	876	855	858	859
11.4	876	854	856	857
12.7	878	856	858	856
14.0	877	855	853	853
15.2	878	855	854	855
16.5	874	---	855	857
17.8	877	850	---	---
19.0	878	---	---	---
20.3	876	---	852	854
21.6	---	---	---	---
22.9	874	---	853	854
24.1	874	853	857	---
25.4	874	850	852	852
26.7	876	---	855	---
27.9	876	854	854	851
29.2	876	---	850	---
30.5	878	848	---	854
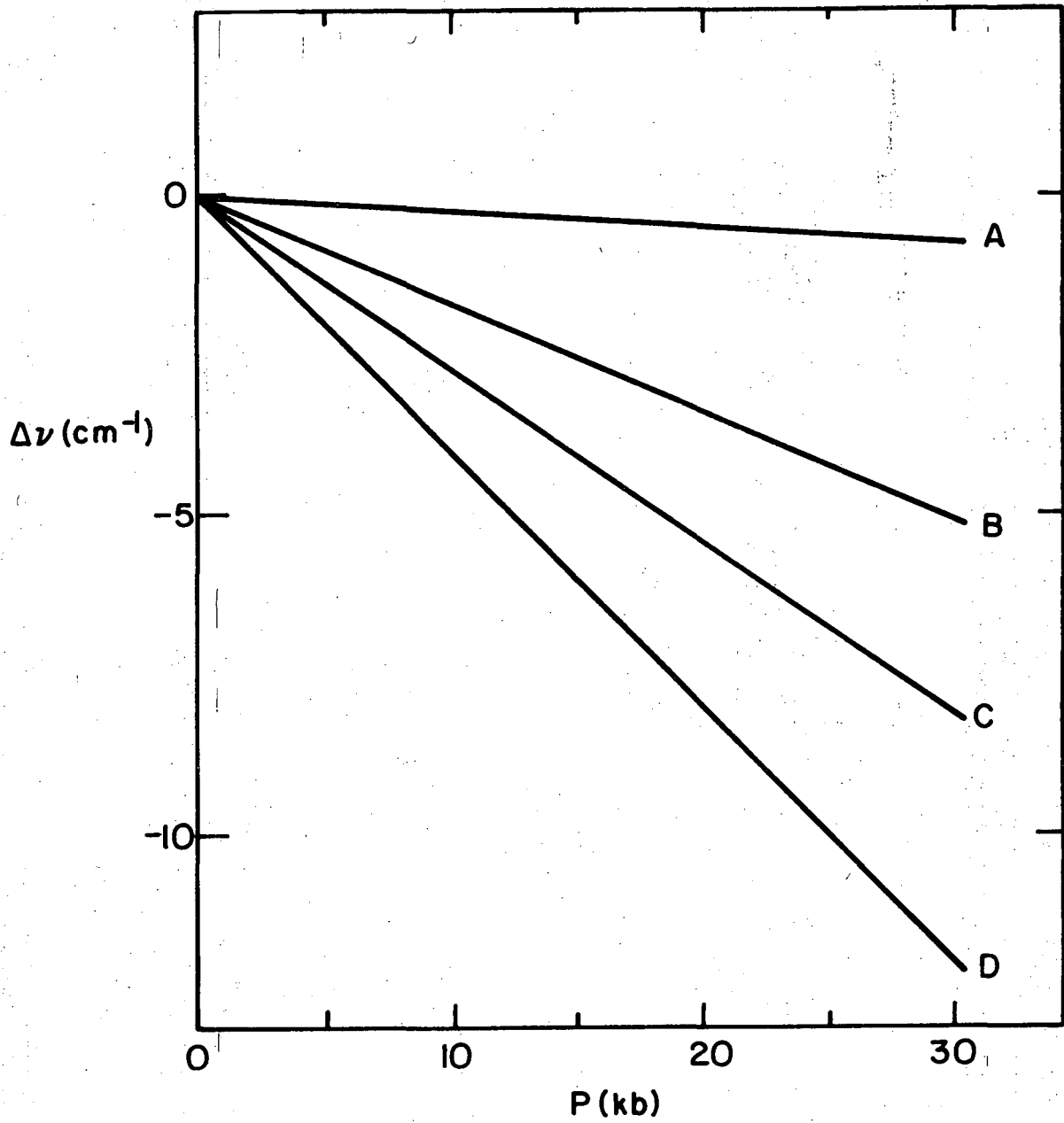
XBL 748-7092

Fig. 21. Shift of out-of-plane bending frequencies with
pressure for some alkaline earth carbonates.
A – Calcite   C – Witherite
B – Strontianite   D – Aragonite

with the experimental results of Weir et al.[92] We see no evidence

of phase transitions in the calcite spectra.* The out-of-plane bends

in natural strontianite, witherite and aragonite are strongly affected

by pressure to 30 kb. Significantly, the shifts are all to lower

frequencies, indicating a negative value for the dipole lattice sums

[Eq. (3)].

Using the measured shifts of absorption frequency due to pressure,

we calculate the interaction terms, F', at atmospheric pressure and at

10 kb. The calculated F' values afford a way to obtain the transition

dipole moments, μ, for the vibrations. F' and μ are shown in Table XIII

for all four of the carbonates studied. Our transition moments are

compared with those of Decius,[7] and agree closely.

The calculated force constant corrections, F', at one atmosphere

and at 10 kb, allow us to calculate R, the nearest neighbor separation

at the higher pressure. From these values of R, we calculate the aver-

age linear compressibilities for aragonite, strontianite, witherite and

calcite along the direction perpendicular to the planes of the carbonate

ions, and show them below.

$$-\frac{1}{L_o}\frac{\Delta L}{\Delta P}$$

aragonite	6.6×10^{-6} bar^{-1}
strontianite	3.0×10^{-6}
witherite	3.5×10^{-6}
calcite	4.4×10^{-6}

---

*Bridgman, in 1939, discovered two other phases of calcium carbonate by
compressing calcite isothermally at room temperature.[93] Fong and Nicol
detected phase transitions of calcite to $CaCO_3$ II (14 kb) and to $CaCO_3$ III
(18 kb) by investigating $CaCO_3$ lattice modes using Raman scattering.

Table XIII.   Inorganic carbonates

	$\nu(\text{cm}^{-1})$*	F'(dyne/cm)	μ (debye/A)	μ (ref.7)
1 atmosphere				
Aragonite	861	-0.0296×10^5	1.9	1.6
Strontianite	858	-0.0352×10^5	2.2	1.8
Witherite	857	-0.0360×10^5	2.5	1.9
Calcite	877	-0.0035×10^5	1.5	---
10 kb				
Aragonite	857	-0.0360×10^5	1.9	
Strontianite	856	-0.0385×10^5	2.2	
Witherite	854	-0.0401×10^5	2.5	
Calcite	876(.8)	-0.0040×10^5	1.5	

*Frequencies are read from the line least-squares-fit to the raw data.

Linear compressibility data on the inorganic carbonates is scarce. Bridgman[94] measured linear compressibilities of calcite. Parallel and perpendicular to the long rhombohedral axis, his linear compressibilities were 0.8×10^{-6} bar^{-1} and 0.3×10^{-6} bar^{-1}, respectively. There are no linear compressibility measurements on aragonite, strontianite or witherite. Comparison of our value of linear compressibility with those of Bridgman shows a discrepancy of a factor of about five. Actually, this is surprising agreement, since $\Delta \nu / \Delta P$ for calcite is so small and absolute errors in determining ν at any pressure are magnified in our calculations.

Madelung and Fuchs[95,96] measured average compressibilities for aragonite, strontianite and witherite and found that compressibilities increased with the size of the cation from 1.5×10^{-6} bar^{-1} to about 2×10^{-6} bar^{-1}. Again our calculated compressibility values disagree, but are still of the same order of magnitude.

The largest contributing factor to the discrepancy between calculated and measured compressibilities appears to be the uncertainty to which the out-of-plane bending frequencies can be measured. But our data illustrate the fact that optical data can be used in determining bulk properties of materials.

While our present calculations give only "order of magnitude" accuracy, we feel that improved high pressure-infrared techniques and more accurately determined dipole lattice sums could not help but give better results.

In conclusion, we have

1. measured the infrared spectra of TCB and DCB as functions of
    pressure to 30 kb,

2. studied the carbonate ion out-of-plane bending frequencies of
    alkaline earth carbonates to 30 kb,

3. justified the consideration of TCB as a one dimensional solid
    and DCB as a two dimensional solid, as far as vibrational proper-
    ties are concerned (similar models have been used in the study
    of energy transfer processes within TCB and DCB[97]),   and

4. shown that the calculation of bulk properties of materials, using
    high pressure-infrared data, is a promising area of study.

ACKNOWLEDGEMENTS

It is impossible to thank everyone involved in the completion
of this thesis. However, I would like to acknowledge, in particular,
Professor George Jura, my associates Tang-hua Chen and Berado Jurado,
and my personal friends Joe Masaryk, Jim Wurzbach and Renee Klang.

REFERENCES

1. A. S. Davydov, _Theory of Molecular Excitons_ [translated by M. Kasha and M. Oppenheimer] (McGraw-Hill, N. Y., 1962), p. 19.

2. D. Craig and P. Hobbins, J. Chem. Soc.   539 (1955).

3. D. Fox and O. Schnepp, J. Chem. Phys. _23_, 767 (1955).

4. R. M. Hexter, J. Chem. Phys. _33_, 1833 (1960).

5. P. P. Ewald, Ann. Phys. Lpz. _64_, 253 (1921).

6. H. Kornfeld, Z. Phys. _22_, 27 (1924).

7. J. C. Decius, J. Chem. Phys. _23_, 1290 (1955).

8. A. S. Davydov, op. cit. (1962).

9. D. Craig and S. Walmsley, _Excitons in Molecular Crystals_ (W. A. Benjamin, Inc., 1968).

10. J. Frenkel, Phys. Rev. _37_, 17 (1931).

11. J. Frenkel, Phys. Rev. _37_, 1276 (1931).

12. S. Bhagavantam and T. Venkatarayudu, Proc. Ind. Acad. Sci. _9_, 224 (1939).

13. D. F. Hornig, J. Chem. Phys. _16_, 1063 (1948).

14. H. Winston and R. Halford, J. Chem. Phys. _17_, 607 (1949).

15. D. Craig and P. Hobbins, op. cit. (1955).

16. D. Fox and O. Schnepp, op. cit. (1955).

17. E. B. Wilson, J. C. Decius and P. Cross, _Molecular Vibrations_ (McGraw-Hill, N. Y., 1955), p. 15.

18. K. Machida and J. Overend, J. Chem. Phys. _51_, 2537 (1969).

19. N. Jacobi, J. Chem. Phys. _57_, 2505 (1972).

20. N. Jacobi and O. Schnepp, J. Chem. Phys. _57_, 2516 (1972).

21. J. R. Scherer and J. C. Evans, Spectrochim. Acta 19, 1739 (1963).

22. G. Herzberg, Molecular Spectra and Molecular Structure. II
    (Van Nostrand, N. J., 1945) p. 178 ff.

23. M. Donoghue, P. H. Hepburn and S. D. Ross, Spectrochim. Acta 27A,
    1065 (1971).

24. J. Rosenthal and G. Murphy, Rev. Mod. Phys. 8, 317 (1936).

25. M. Tinkham, Group Theory and Quantum Mechanics (McGraw-Hill, N. Y.,
    1964) p. 238 ff.

26. International Tables for X-ray Crystallography Vol. I (Kynoch Press,
    London, 1952) p. 10.

27. D. F. Hornig, op. cit. (1948).

28. R. S. Halford, J. Chem. Phys. 14, 8 (1946).

29. L. Couture, J. Chem. Phys. 15, 153 (1947).

30. H. Winston, J. Chem. Phys. 19, 156 (1951).

31. R. M. Hexter, op. cit. (1960).

32. C. Kittel, Introduction to Solid State Physics, 4th Edition
    (John Wiley & Sons, N. Y., 1971) p. 305.

33. C. Kittel, ibid., p. 180.

34. P. A. Reynolds, J. K. Kjems and J. W. White, J. Chem. Phys. 56,
    2928 (1972).

35. D. L. Swanson and D. A. Dows, Chem. Phys. Lett. 23, 430 (1973).

36. M. Lax and E. Burstein, Phys. Rev. 97, 39 (1955).

37. D. P. Craig and V. Schettino, Chem. Phys. Lett. 23, 315 (1973).

38. A. S. Davydov, op. cit. (1962) p. 19.

39. R. Ladenburg, Z. Phys. 4, 151 (1921).

40. A. S. Davydov, op. cit. (1962), p. 21.

41. R. M. Hexter, op. cit. (1960).

42. E. Fishman and H. G. Drickamer, Anal. Chem. $\underline{28}$, 804 (1956).

43. C. E. Weir, A. Valkenburg and E. R. Lippincott, J. Res. Nat. Bur. Std. $\underline{63A}$, 55 (1959).

44. E. R. Lippincott, C. E. Weir, A. Van Valkenburg and E. N. Bunting, Spectrochim. Acta $\underline{16}$, 58 (1960).

45. G. Jura, private communication.

46. A. S. Balchan and H. G. Drickamer, Rev. Sci. Instr. $\underline{31}$, 511 (1960).

47. M. Nicol, J. Opt. Soc. Am. $\underline{55}$, 1176 (1965).

48. Y. Ebisuzaki, and M. Nicol, Chem. Phys. Lett. $\underline{3}$, 480 (1969).

49. J. R. Ferraro, S. S. Mitra and C. Postmus, Inorg. Nucl. Chem. Lett. $\underline{2}$, 269 (1966).

50. C. Postmus, J. R. Ferraro and S. S. Mitra, Inorg. Nucl. Chem. Lett. $\underline{4}$, 55 (1968).

51. C. C. Bradley, H. A. Gebbie, A. C. Gilby, V. V. Kechin and T. H. King, Nature $\underline{211}$, 839 (1966).

52. W. F. Sherman, J. Sci. Instr. $\underline{43}$, 1462 (1966).

53. M. Nicol, Y. Ebisuzaki, W. Ellenson and A. Karim, Rev. Sci. Instr. $\underline{43}$, 1368 (1972).

54. P. W. Bridgman, Rev. Mod. Phys. $\underline{18}$, 1 (1946).

55. W. D. Buckingham and C. R. Deibert, J. Opt. Soc. Amer. $\underline{36}$, 245 (1946).

56. G. C. Turrell, J. Opt. Soc. Amer. $\underline{52}$, 771 (1962).

57. C. K. Wu, Ph.D. dissertation, University of California, Berkeley (1971).

-83-

58. R. R. Wiederkehr and H. G. Drickamer, J. Chem. Phys. $\underline{28}$, 311 (1958).

59. J. F. Assel and M. Nicol, J. Chem. Phys. $\underline{49}$, 5395 (1968).

60. M. Nicol, Y. Ebisuzaki, W. Ellenson and A. Karim, op. cit. (1972).

61. M. Y. Fong and M. Nicol, op. cit. (1971).

62. P. W. Bridgman, Proc. Amer. Acad. Arts Sci. $\underline{76}$, 55 (1948).

63. H. L. Davies, J. Res. Natl. Bur. Std. $\underline{72A}$, 149 (1968).

64. C. K. Wu, op. cit. (1971).

65. C. Dean, M. Pollak, B. M. Craven and G. A. Jeffrey, Acta Cryst. $\underline{11}$, 710 (1958).

66. G. Gafner and F. H. Herbstein, Acta Cryst. $\underline{17}$, 1094 (1964).

67. U. Croatto, S. Bezzi and E. Bua, Acta Cryst. $\underline{5}$, 825 (1952).

68. F. H. Herbstein, Acta Cryst. $\underline{18}$, 997 (1965).

69. S. Saeki, Bull. Chem. Soc. Japan $\underline{34}$, 1858 (1961).

70. J. R. Scherer, Spectrochim. Acta $\underline{19}$, 601 (1963).

71. J. R. Scherer and J. C. Evans, Spectrochim. Acta $\underline{19}$, 1739 (1963).

72. A. Stojiljkovic and D. H. Whiffen, Spectrochim. Acta $\underline{12}$, 47 (1958).

73. E. A. D'Alessio and H. Bonadeo, Chem. Phys. Lett. $\underline{22}$, 559 (1973).

74. P. A. Reynolds, J. K. Kjems and J. W. White, op. cit. (1972).

75. P. P. Ewald, op. cit. (1921).

76. R. M. Hexter, J. Chem. Phys. $\underline{37}$, 1347 (1962).

77. B. R. Nijboer and F. W. deWette, Physica $\underline{24}$, 422 (1958).

78. J. C. Decius, O. G. Malan and H. W. Thompson, Proc. Roy. Soc. $\underline{275A}$, 295 (1963).

79. P. W. Bridgman, Proc. Amer. Acad. Arts Sci. $\underline{76}$, 1 (1945).

80. R. W. G. Wyckoff, Crystal Structures (J. Wiley & Sons, Inc., N. Y., 1969) v. 6, p. 94 ff.

81. J. R. Scherer and J. C. Evans, Op. Cit. (1963).

82. E. A. D'Alessio and H. Bonadeo, op. cit. (1973).

83. P. W. Bridgman, op. cit. (1945).

84. J. C. Decius, J. Chem. Phys. $\underline{22}$, 1941 (1954).

85. J. C. Decius, J. Chem. Phys. $\underline{22}$, 1946 (1954).

86. J. C. Decius, J. Chem. Phys. $\underline{23}$, 1290 (1955).

87. W. L. Bragg and G. F. Claringbull, Crystal Structure of Minerals (G. Bell, London, 1965).

88. J. C. Decius, O. G. Malan and H. W. Thompson, op. cit. (1963).

89. P. P. Ewald, op. cit. (1921).

90. G. Herzberg, op. cit. (1945) p. 178.

91. J. C. Decius, op. cit. (1955).

92. C. E. Weir, E. R. Lippincott, A. Van Valkenburg and E. N. Bunting, op. cit. (1959).

93. P. W. Bridgman, Proc. Amer. Acad. Arts Sci. $\underline{76}$, 55 (1948).

94. P. W. Bridgman, Am. J. Sci. $\underline{10}$, 483 (1925).

95. E. Madelung and R. Fuchs, Ann. Phys. $\underline{65}$, 289 (1921).

96. D. F. Eggers and B. L. Crawford, J. Chem. Phys. $\underline{19}$, 1554 (1951).

97. M. D. Fayer, private communication.